NANYANG TECHNOLOGICAL UNIVERSITY
SINGAPORE

DOA ESTIMATION METHODS WITH UNKNOWN NUMBER OF SOURCES

WANG ZHIZHENG

SCHOOL OF ELECTRICAL & ELECTRONIC ENGINEERING

2020

DOA ESTIMATION METHODS WITH UNKNOWN NUMBER OF SOURCES

WANG ZHIZHENG

School of Electrical & Electronic Engineering

A thesis submitted to the Nanyang Technological University
in partial fulfillment of the requirement for the degree of
Master of Engineering

2020

Statement of Originality

I hereby certify that the work embodied in this thesis is the result of original research, is free of plagiarised materials, and has not been submitted for a higher degree to any other University or Institution.

09-03-20

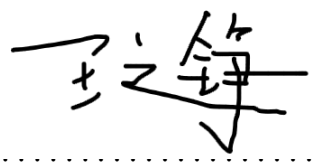

. . . . . .

Date

. . . . . .

WANG ZHIZHENG

Supervisor Declaration Statement

I have reviewed the content and presentation style of this thesis and declare it is free of plagiarism and of sufficient grammatical clarity to be examined. To the best of my knowledge, the research and writing are those of the candidate except as acknowledged in the Author Attribution Statement. I confirm that the investigations were conducted in accord with the ethics policies and integrity standards of Nanyang Technological University and that the research data are presented honestly and without prejudice.

09-03-20

. . . . . .

Date

. . . . . .

NG BOON POH

Authorship Attribution Statement

Please select one of the following; *delete as appropriate:

*(A) This thesis **does not** contain any materials from papers published in peer-reviewed journals or from papers accepted at conferences in which I am listed as an author.

~~*(B) This thesis contains material from 0 paper(s) published in the following peer-reviewed journal(s) / from papers accepted at conferences in which I am listed as an author.~~

09-03-20

. . . . . .
Date

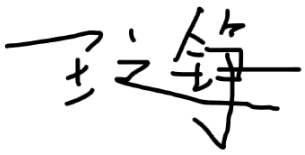

. . . . . .
WANG ZHIZHENG

Acknowledgements

There is an old saying in Chinese culture, ‘The one must suffer physically and mentally for what to be gained as will and knowledge.’ There were many unfortunate personal tragedies happened during my Master of Engineering candidature. I have this sentence in my heart, but they were even more than I could bear. The only support that carried me through this hard time is from my supervisor Assoc Prof. Ng Boon Poh. There is no way for me finish the research without him. His professional guidance is clear, inspiring and wise. Besides of that, he also takes good care of my mental health gently and carefully. His help is more than just an academic supervisor but also a guide of life. There is no literature could express my gratitude and appreciation to Prof Ng.

I would also like to thank Dr. Narong Borijindargoon and PhD student S Supraja. Their insight opinions and friendship helped me get passed many difficulties academic-wise and personal-wise.

Last but not least, I would like to thank Mr. Melvin Tan and Mr. Lim Cheng Chye who are the staff from Information System Research Lab for their patient technical support.

Table of Contents

List of Figures

List of Tables

Summary

Direction of arrival (DoA) estimation is a major topic investigated in smart antenna and array signal processing area of wireless communication. It is closely linked to source localization which provides the spatial information of the signal sources. DoA estimation algorithms make it possible to receive signal from a particular direction and suppress noises from other directions.

The main targets of this project are:

1. Improve the performance of conventional MUSIC algorithm in terms of computational complexity.
2. Propose a new high-resolution estimation method without the information of number of signal sources.
3. Provide wideband solutions for the new algorithm with wideband adoption methods.

The conventional MUSIC algorithm is studied and interpreted as a MVDR estimator with infinite input signal power. An alternative high-resolution DoA estimation method is introduced based on this interpretation. Instead of signal power, the noise power is now set to be negative infinite in dB. Subsequently, the scanning method in the conventional MUSIC algorithm is re-designed in order to reduce the computational load. The new scanning method takes advantage of the relationship between spectrum parameters and the number of array elements in order to minimize the number of direction scans while remain the quality of resolution.

The new Unity-Response-Like (UR-Like) high-resolution estimation method without number of sources is proposed and examined with numerical simulations. The idea behind the UR-Like algorithm is to maintain the difference between array response and unity over the field of view while minimizing the mean output power. The UR-Like algorithm is also compared with a competitive algorithm, the MUSIC-Like algorithm. With the same design requirement of high-

resolution DoA estimation method without number of sources, the UR-Like has the advantage of less computational load against the MUSIC-Like algorithm. Last but not least, the UR-Like algorithm is extended to wideband scenarios with the help of the frequency scanning and the Taylor series methods. The Taylor series method is later applied to the MUSIC-Like and the MVDR algorithms for wideband extension as well.

Chapter 1 Introduction

1.1 Background and Motivation

The wireless communication industry has grown strongly over the past few decades. Electronic devices are becoming smaller and more wireless. The trend of Internet of things and smart nation requires a reliable connection of all devices and sensors through wireless communication. Direction of arrival (DoA) estimation is a major topic investigated in smart antenna and array signal processing area of wireless communication genus. DoA estimation is closely linked to source localization which provides the spatial information of the signal sources and makes it possible to receive signal from a particular direction and suppress noises from other directions. Its ability of transmitting and receiving signal power towards an interested direction has been an effective tool in many fields like smart antenna, medical diagnosis, jamming signal cancellation, etc.

The techniques of DoA estimation fall into the area of array signal processing. Sensor arrays have been used for many practical signal processing applications. The data collected by sensor arrays contains many properties and parameters of the signal such as power level and direction of arrival. DoA estimation algorithms are designed to reveal the spatial property. Many well-known algorithms have been investigated and practically implemented in many applications [1], such as:

- Capon's Minimum Variance Distortionless (MVDR) method
- Multiple Signal Classification (MUSIC) algorithm
- Unity-Response (UR) algorithm
- MUSIC-Like algorithm

They are introduced and studied through references [2] to [8]. Both conventional and subspace processing techniques have various pros and cons for different application requirements. The balance among resolution of performance, estimation accuracy, robustness and computational complexity is always an issue to be addressed.

1.2 Motivation

In many application scenarios, the number of signal sources is an unknown information for the sensor array, yet the algorithm still needs to estimate the direction of arrival. Super resolution techniques like the MUSIC and UR algorithms need a prior knowledge of number of sources to perform DoA estimation which limits their robustness. On the other hand, conventional method like the MVDR does not require number of sources as input to estimate DoA. However, the resolution of outcome is poor compare to subspaces techniques.

Moreover, most of the DoA estimation methods are proposed for narrowband scenarios only. However, the wideband signals are equally important in real-life applications. In fact, wideband solution for DoA estimation is necessary for many sonar, radar and wireless communication applications.

Speaking of real-life applications, the computational complexity is also an important criterion to evaluate the efficiency of an algorithm. It is always a good thing to save more computational resources while maintaining the same resolution and accuracy.

1.3 Objectives

Motivated by the necessity of fast, high-resolution DoA estimation solution without number of sources, the objectives of this project are therefore:

1. To study and compare existing DoA estimation algorithms, verify their effectiveness and the linkage among them.
2. To study the nature of MUSIC algorithm and find out an alternative high-resolution algorithm and computational complexity reduction method making use of some properties of the MUSIC algorithms.
3. To find out a high-resolution solution without number of sources.
4. To extend the new algorithm to wideband scenarios.

1.4 Major Contribution of the Thesis

The main contributions of this thesis are as follows:

1. A high-resolution DoA estimation method is proposed based on the linkage between the MVDR and MUISC algorithms. This algorithm is designed to deliver high-resolution spectrum while keeping the true power of the signal of interest. Its performance and limitations are studied based on computer simulation.
2. A scanning method is introduced for the MUSIC algorithm to reduce its computational complexity. The improved scanning method is an application of the nature of the MUSIC spatial spectrum. Statistical performance is studied comparing to the conventional scan

method. This method is able to reduce the number of scan by more than half of it while not missing or degrading any directional estimation.

3. A new high-resolution DoA estimation method without the number of sources is proposed and named as the UR-Like algorithm. The algorithm exploits the principle of the MVDR and UR algorithms. The UR-Like algorithm is able to deliver a high-resolution result similar to the UR algorithm but does not require the information of number of sources, like the MVDR algorithm. Statistical performance is analyzed as well focusing on its estimation accuracy, resolution capability and computational complexity. It also has advantage in computational complexity against competitive algorithm, the MUSIC-Like algorithm.
4. Two methods are employed to extend the UR-Like algorithm into wideband. Frequency scanning method is an extension of the idea of the UR-Like algorithm in frequency domain. The other method makes use of the Taylor expansion to infuse frequency component into the data covariance matrix, so that the wideband signal could be detected in only 1-time directional scanning. The Taylor series method is also introduced to the MVDR and the MUSIC-Like algorithm for wideband adoption.

1.5 Organization of the Report

This thesis consists of 7 chapters. In Chapter 2, fundamentals of array signal processing are introduced along with the data model. Meanwhile, terms and notations mentioned frequently are introduced. A review of typical and classic DoA estimation methods focused in this thesis is also provided in Chapter 2. In Chapter 3, an alternative algorithm using the nature of MUSIC algorithm is proposed with statistical performance analysis. In Chapter 4, an improved scanning method designed for the MUSIC algorithm is introduced. The computational complexity comparison between the improved and conventional methods is proved based on computer simulations. In

Chapter 5, a high-resolution DoA estimation algorithm without number of sources which links to the UR method is proposed with detailed statistical performance analysis. Chapter 6 includes 2 methods used for wideband extension for the UR-Like algorithm, the frequency scanning method and the Taylor series method. The Taylor series method is also employed to the MVDR and the MUSIC-Like algorithms in this chapter. Last but not least, Chapter 7 concludes this thesis and makes recommendations for future works.

Chapter 2 Principles and Reviews

2.1 Array Signal Processing

Array signal processing techniques make use of multiple sensor elements and the complex weight assigned to each element to perform some specific processing purposes. Digital Beamforming is one of the practical implementations of such idea. Beamforming technology is a spatial filtering process which manipulates the weight vectors according to beamforming algorithms which refer to the received sensor array data. The weight vector shapes the overall array beam pattern to meet requirement for different applications. Direction of arrival (DoA) estimation is one of the major topics in array processing technology. A simple illustration of array signal processing structure is shown in Figure 2.1.

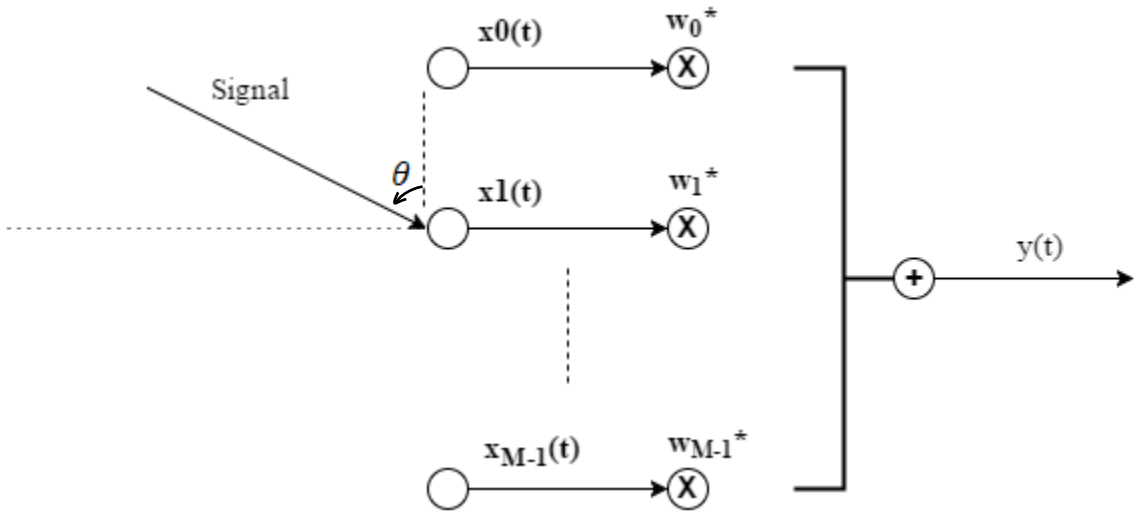

Figure 2.1: Array Signal Processing Structure

According to Figure 2.1, the output of each sensor is multiplied by complex weight vector with both amplitude and phase then summed up together as the overall array output. The mathematical expression is given by:

$$y(t) = \sum_{m=0}^{M-1} x_m(t) w_m^* \tag{2.1.1}$$

where superscript * denotes complex conjugate, m is the channel index number.

The lineup of the sensor elements in an array may have different configurations. The array geometry is a study of element lineup configuration. A proper array geometry defines the reference of signal direction and add dimensions into the acquisition space. However, there is no one perfect geometry that fits perfectly for every signal environment. The most popular array geometries are linear and circular arrays. In this report, a Uniform Linear Array (ULA) geometry will be taken as it is the most common basic array geometry. The ULA is defined with an inter-element-space of half of the wavelength of the interested signal to avoid spatial aliasing.

2.2 Array Response and Output Power Model

After choosing the array geometry, the mathematical expression of an array output could be used to derive the array response. Assume that the ULA consists of M identical sensors and there are K uncorrelated narrowband signal sources to be detected. The received signal at the m^{th} sensor is:

$$x_{\mathrm{m}}(t) = \sum_{k=0}^{K-1} a_k(t)\, e^{j\pi d_m cos\theta_k} + n_{\mathrm{m}}(t). \tag{2.2.2}$$

In this equation, $a_k(t)$ represents the signal data from the k^{th} source. d_m represents the normalized sensor position with respect to inter-element-space and half-wavelength. θ_k represents

the DoA of the k^{th} source with respect to reference array axis. $n_{\mathrm{m}}(t)$ represents the stationary zero-mean stochastic additive noise at the m^{th} sensor with a variance of σ_n^2.

Considering $\mathbf{x}(t)$ as the M*1 vector that contains the received data of all sensors:

$$\mathbf{x}(t) = \sum_{k=0}^{K-1} a_k(t)\, \mathbf{s}(\theta_k) + \mathbf{n}(t). \tag{2.2.3}$$

Vector $\mathbf{s}(\theta)$ is defined as the Steering Vector (SV) which is a direction vector related to DoA:

$$\mathbf{s}(\theta_k) = \left[e^{j\pi d_0 cos\theta_k}, e^{j\pi d_1 cos\theta_k}, \cdots, e^{e^{j\pi d_{M-1} cos\theta_k}}\right]^T. \tag{2.2.4}$$

Vector $\mathbf{n}(t)$ is the collection of noises:

$$\mathbf{n}(t) = [n_0(t), n_1(t), \cdots, n_{\mathrm{M}-1}(t)]^T . \tag{2.2.5}$$

Considering a unity input without noises, the array response could be found as the sum of all weighted:

$$\mathbf{H}(\theta) = \sum_{m=0}^{M-1} \mathbf{s}(\theta) w_m^* = \mathbf{w}^H \mathbf{s}(\theta) \tag{2.2.6}$$

where superscript *H* refers to complex conjugate transpose.

The weight vector $\mathbf{w}$ contains the M complex conjugate coefficients of each channel given by:

$$\mathbf{w} = [w_0, w_1, \cdots, w_{M-1}]^T \tag{2.2.7}$$

where superscript *T* refers to vector or matrix transpose.

The output power of the array system is

$$\mathbf{P} = E[|y(t)|^2] = \mathbf{w}^H E[x(t)x^H(t)]\mathbf{w} = \mathbf{w}^H \mathbf{R}\mathbf{w} \tag{2.2.8}$$

where E[·] is the expectation operator.

R is the received array data covariance matrix of the incoming signal:

$$\mathbf{R} = \mathbf{S}\mathbf{R}_s\mathbf{S}^H + \sigma_n^2\mathbf{I} \tag{2.2.9}$$

where **I** is a M*M identity matrix and:

$$\mathbf{S} = [\mathbf{s}(\theta_0), \mathbf{s}(\theta_1), \cdots, \mathbf{s}(\theta_{K-1})] \tag{2.2.10}$$

$$\mathbf{R}_s = E[\mathbf{a}(t)\mathbf{a}^H(t)] \tag{2.2.11}$$

$$\mathbf{a}(t) = [a_0(t), a_1(t), \cdots, a_{K-1}(t)]^T. \tag{2.2.12}$$

The covariance matrix **R** can be eigen-decomposed into signal subspace $\{\mathbf{E}_s, \boldsymbol{\Lambda_s}\}$ and noise subspace $\{\mathbf{E}_n, \boldsymbol{\Lambda_n}\}$ because it is Hermitian and positive definite (power is always nonnegative).

$$\mathbf{R} = \mathbf{E}\boldsymbol{\Lambda}\mathbf{E}^H = \mathbf{E}_s\boldsymbol{\Lambda_s}\mathbf{E}_s^H + \mathbf{E}_n\boldsymbol{\Lambda_n}\mathbf{E}_n^H \tag{2.2.13}$$

where

$$\mathbf{E} = [\boldsymbol{\beta}_0, \boldsymbol{\beta}_1, \cdots, \boldsymbol{\beta}_{M-1}] = [\boldsymbol{\beta}_0, \boldsymbol{\beta}_1, \cdots, \boldsymbol{\beta}_{K-1}\, \boldsymbol{\beta}_K, \boldsymbol{\beta}_{K+1}, \cdots, \boldsymbol{\beta}_{M-1}] \tag{2.2.14}$$

where $\boldsymbol{\beta}$ are the eigenvectors and λ are the eigenvalues:

$$\boldsymbol{\Lambda} = \begin{bmatrix} \lambda_0 & \cdots & 0 \\ \vdots & \ddots & \vdots \\ 0 & \cdots & \lambda_{M-1} \end{bmatrix} = diag[\lambda_0, \lambda_1, \cdots, \lambda_{K-1}, \sigma_n^2, \sigma_n^2, \cdots, \sigma_n^2]. \tag{2.2.15}$$

The first K eigenvalues are corresponding to the signal power. Hence signal subspace and noise subspace matrixes are

$$\mathbf{E}_s = [\boldsymbol{\beta}_0\, \boldsymbol{\beta}_1\, \cdots\, \boldsymbol{\beta}_{K-1}] \tag{2.2.16}$$

$$\mathbf{E}_n = [\boldsymbol{\beta}_K\, \boldsymbol{\beta}_{K+1}\, \cdots\, \boldsymbol{\beta}_{M-1}]. \tag{2.2.17}$$

2.3 DoA Estimation Algorithms Review

In this section, three DoA estimation algorithms will be discussed based on the array system model in Section 2.2. They have been widely applied in audio, radar and wireless communication sectors for decades. Besides introducing the fundamental logic of those algorithms, an insight of the relation among those algorithms is also discussed.

DoA estimation algorithms using sensor array could be generally divided into to two categories: conventional and eigenvector-based (also known as subspace) methods. Conventional methods like the Minimum Variance Distortionless Response (MVDR) algorithm make use of the concept of steering vector in equation (2.2.4) for null-steering. Eigenvector-based subspace methods like the Multiple Signal Classification (MUSIC) algorithm take advantage of statistical model of the received signal in equation (2.2.9) to perform an estimation with higher resolution.

2.3.1 Capon's Minimum Variance Distortionless Response (MVDR) Algorithm

Capon's Minimum Variance Distortionless Response (MVDR) algorithm finds the maximum likelihood estimation of the power of interested signals from their directions, which means to form a beam pointing towards the looking direction while nulls the directions of interference. This method uses the array weights, which are obtained by minimizing the mean output power subject to unity constraint in the look direction. This idea could be translated into a constrained optimization problem [9]:

$$\min_{\mathbf{w}} \ \mathbf{w}^H \mathbf{R} \mathbf{w} \tag{2.3.18}$$

$$s.t\ \mathbf{w}^H \mathbf{s}_\theta = 1 \tag{2.3.19}$$

where $\mathbf{s}_\theta$ is the steering vector $\mathbf{s}(\theta, \omega)$ for a certain frequency ω.

Using the Lagrange multiplier method, the weight vector for the MVDR algorithm could be solved as:

$$\mathbf{w}_{MVDR} = \frac{\mathbf{R^{-1}s}_\theta}{\mathbf{s}_\theta^H \mathbf{R^{-1}s}_\theta}. \tag{2.3.20}$$

The direction-finding function is the power spectrum of the array which could be expressed as

$$DF_{MVDR} = \mathbf{w}^H \mathbf{R w} = \frac{1}{\mathbf{s}_\theta^H \mathbf{R^{-1}s}_\theta}. \tag{2.3.21}$$

By applying this optimization problem to every angle of the Field of View (FoV) of the array geometry, the peak of the total power spectrum plot indicates the DoA.

The MVDR method maximizes the output SNR while keeping the amplitude of interested signals from known directions unchanged because of the unity constraint. It also bears some disadvantages as well. Firstly, The MVDR method is not applicable for correlated signals because the correlated components may be combined destructively in the process of minimizing the output power. Secondly, the MVDR method has trouble in distinguishing closely-situated sources, since the minimizing process between two close sources would not be significant. Thirdly, the MVDR method computes the inverse of covariance matrix, which might be a huge computational load for large data scale. Fourthly, the MVDR has relatively better resolution than other types of conventional algorithms, like Delay-and-Sum, its resolution capability is still not optimized, especially comparing to eigenvector-based subspace algorithms [10].

2.3.2 Multiple Signal Classification (MUSIC) Algorithm

The Multiple Signal Classification (MUSIC) method is an eigenvector-based subspace algorithm. It estimates the noise subspace by eigenvalue decomposition of the array covariance matrix. Once the noise subspace has been estimated, a search for directions is made by looking for the steering vectors that are as orthogonal to the noise subspace as possible.

$$\mathbf{s}_\theta^H \mathbf{E}_n \mathbf{E}_n^H \mathbf{s}_\theta = \mathbf{0}\,. \tag{2.3.22}$$

For all the steering vectors $\mathbf{s}_\theta$ which has zero projection into the noise subspace reveal the signal directions. To form a positive-peak beam plot, the direction-finding function is the inverse of the expression in equation (2.3.22):

$$DF_{MUSIC} = \frac{1}{\mathbf{s}_\theta^H \mathbf{E}_n \mathbf{E}_n^H \mathbf{s}_\theta}\,. \tag{2.3.23}$$

Such an idea could also be translated into the following optimization problem [4]:

$$\min_{\mathbf{w}} \; ||\mathbf{w} - \mathbf{s}_\theta||^2 \tag{2.3.24}$$

$$s.t\; \mathbf{E}_s^H \mathbf{w} = 0 \tag{2.3.25}$$

where $\mathbf{E}_s^H$ is the single subspace matrix of incoming signal containing all signal eigenvectors.

Using Lagrange multiplier method, the weight vector for the MUSIC algorithm could be solved as:

$$\mathbf{w}_{MUSIC} = \mathbf{E}_n \mathbf{E}_n^H \mathbf{s}_\theta\,. \tag{2.3.26}$$

The direction-finding function is the inverse of array response which could be expressed as

$$DF_{MUSIC} = \frac{1}{\mathbf{w}_{MUSIC}^H \mathbf{s}(\theta)} = \frac{1}{\mathbf{s}_\theta^H \mathbf{E}_n \mathbf{E}_n^H \mathbf{s}_\theta} = \frac{1}{||\mathbf{E}_n^H \mathbf{s}_\theta||^2}\,. \tag{2.3.27}$$

Equation (2.3.27) and equation (2.3.23) are exactly the same.

Instead of the true value of the signal source, the peaks of the MUSIC spatial spectrum are theoretically set to be infinity. Because the orthogonality between signal steering vector and noise subspace will minimize the denominator in the direction-finding function and hence will give rise to the infinite high peaks in the MUSIC spectrum to indicate the DoA. The Signal-to-Noise Ratio (SNR) is larger than that of MVDR.

Unlike the conventional methods, the MUSIC spatial spectrum does not estimate the signal power associated with each arrival angle. Instead, when the ensemble average of the array input covariance matrix is known exactly, under uncorrelated and identical noise conditions, the peaks of the direction-finding function of the MUSIC are guaranteed to correspond to the true directions of arrival. Since these peaks are distinct irrespective of the actual separation between arrival angles, in principle, with perfect array calibration, the MUSIC algorithm is able to distinguish and resolve closely-situated signals [10].

2.3.3 Unity Response (UR) Algorithm

The Unity Response (UR) method minimizes the mean-square value of the difference between actual array response and unity response in the interested directions while applying nulling directional eigenvector constraints to the signal subspace. Such an idea could be translated into the following optimization problem [5]:

$$\min_{\mathbf{w}} \int ||\mathbf{w}^H \mathbf{s}_\theta - \mathbf{1}||^2 \, d\boldsymbol{\theta} \tag{2.3.28}$$

$$s.t\ \mathbf{E}_s^H \mathbf{w} = 0\ . \tag{2.3.29}$$

The direction-finding function is the inverse of the array response which could be expressed as

$$DF_{UR} = \frac{1}{|\mathbf{w}_{UR}^H \mathbf{s}_\theta|^2}. \tag{2.3.30}$$

The UR algorithm is a high resolution DoA estimation method using subspace methods. Its performance is dependent on the range of integration in equation (2.3.28). When the integration covers the full Field of View (FoV) of the array geometry, the performance of the UR algorithm approaches to the Minimum-Norm algorithm. When the integration focuses on smaller region, saying every bearing angle, the performance would approach to the MUSIC algorithm. Generally speaking, the UR algorithm is an algorithm between the MUSIC and MN algorithms.

2.3.4 MUSIC-Like Algorithm

The MUSIC-Like algorithm proposed in [7] is a new DoA estimation method realized in the beamforming framework. It aims to minimize the mean array output power subject to retaining the output power at the looking direction. Unlike the distortionless response of MVDR algorithm, the MUSIC-Like algorithm focuses more on the output power than output signal itself. Hence the constraint of MUSIC-Like algorithm is on the square of the gain at each look direction, instead of unity, with an L_2 norm constraint on the weight vector for a meaningful result.

The optimization problem could be expressed as:

$$\min_{\mathbf{w}} \ \mathbf{w}^H \mathbf{R} \mathbf{w} \tag{2.3.31}$$

$$s.t\ \mathbf{w}^H \mathbf{s}_\theta \mathbf{s}_\theta^H \mathbf{w} + \beta ||\mathbf{w}||^2 = c \tag{2.3.32}$$

where β and c are constants larger than zero.

Apply the Lagrange multiplier method to this problem and define the Lagrange function as:

$$L(\mathbf{w},\lambda) = \mathbf{w}^H\mathbf{R}\mathbf{w} - \lambda\left(\mathbf{w}^H\mathbf{s}_\theta\mathbf{s}_\theta^H\mathbf{w} + \beta||\mathbf{w}||^2 - c\right) \tag{2.3.33}$$

where λ is the Lagrange multiplier.

The gradient of this function with respect to weight vector is:

$$\frac{\partial L}{\partial \mathbf{w}} = \mathbf{R}\mathbf{w} - \lambda\left(\mathbf{s}_\theta\mathbf{s}_\theta^H\mathbf{w} + \beta\mathbf{w}\right). \tag{2.3.34}$$

Setting the gradient to zero yields:

$$\mathbf{R}\mathbf{w} = \lambda\left(\mathbf{s}_\theta\mathbf{s}_\theta^H + \beta\mathbf{I}\right)\mathbf{w}. \tag{2.3.35}$$

The optimal weight vector could be solved as the generalized eigenvector of the matrix pencil $\{\mathbf{R}, \mathbf{s}_\theta\mathbf{s}_\theta^H + \beta\mathbf{I}\}$ associated with its minimum generalized eigenvalue. Such process should be performed for every looking direction for the whole spectrum.

The direction-finding function is the inverse of the power of array response which could be expressed as

$$DF_{MUSIC-Like} = \frac{1}{|\mathbf{w}_{MUSIC-Like}^H\mathbf{s}(\theta)|^2}. \tag{2.3.36}$$

This algorithm is called MUSIC-Like because its quiescent response is identical to the MUSIC algorithm [7]. Its underlying working principle is also similar to that of the MUSIC algorithm [8]. However, unlike the MUSIC algorithm, MUSIC-Like algorithm does not require precise eigen-decomposition in practice, which means that the number of source is not required as a prior knowledge. Instead, the MUSIC-Like algorithm requires generalized eigen-decomposition for every direction. It adds more robustness comparing to the MUSIC algorithm in the cost of computational complexity.

2.4 The Relation Between MVDR and MUSIC

From Section 2.3.1, the direction-finding function of MVDR makes use of the inverse of the covariance matrix, recall the formulation of data covariance matrix from equation (2.2.13) and (2.2.15) under the assumption of uncorrelated additive noise power of σ_n^2:

$$\mathbf{R} = \mathbf{E}\boldsymbol{\Lambda}\mathbf{E}^H = [\mathbf{E}_s\ \mathbf{E}_n]\boldsymbol{\Lambda}\begin{bmatrix}\mathbf{E}_s\\ \mathbf{E}_n\end{bmatrix}, \tag{2.2.13}$$

$$\boldsymbol{\Lambda} = \begin{bmatrix}\lambda_0 & \cdots & 0\\ \vdots & \ddots & \vdots\\ 0 & \cdots & \lambda_{M-1}\end{bmatrix} = diag[\lambda_0, \lambda_1, \cdots, \lambda_{K-1}, \sigma_n^2, \sigma_n^2, \cdots, \sigma_n^2\ ]. \tag{2.2.15}$$

It is assumed that both matrix $\mathbf{E}$ and $\boldsymbol{\Lambda}$ are full rank. Applying the matrix inversion to covariance matrix delivers:

$$\mathbf{R}^{-1} = [\mathbf{E}_s\ \mathbf{E}_n]\boldsymbol{\Lambda}^{-1}\begin{bmatrix}\mathbf{E}_s\\ \mathbf{E}_n\end{bmatrix}. \tag{2.4.37}$$

To increase the performance of MVDR algorithm, the signal power is set to be infinity while the noise power remains as σ_n^2. The SNR approaches to infinity.

When signal power is set to be infinity, the inverse of signal covariance matrix approaches to zero.

$$\mathbf{R}^{-1} = [\mathbf{E}_s\ \mathbf{E}_n]\widehat{\boldsymbol{\Lambda}}^{-1}\begin{bmatrix}\mathbf{E}_s\\ \mathbf{E}_n\end{bmatrix} = \mathbf{E}_n\mathbf{E}_n^H \tag{2.4.38}$$

where $\widehat{\boldsymbol{\Lambda}}^{-1} = diag[[0, 0, \cdots, 0]_K, \sigma_n^{-2}, \sigma_n^{-2}, \cdots, \sigma_n^{-2}\ ]$.

The direction-finding function of the MVDR is now:

$$DF_{MVDR} = \frac{1}{\mathbf{s}_\theta^H\mathbf{E}_n\mathbf{E}_n^H\mathbf{s}_\theta}. \tag{2.4.39}$$

The new spectrum function of MVDR is equal to the one of MUSIC in equation (2.3.27).

Now the MUSIC algorithm could be interpreted as a special case of the MVDR. When applying the MVDR to an infinite SNR data covariance matrix, the performance is the same as that of the MUSIC algorithm. This also explains the higher resolution of MUSIC compare to MVDR.

Chapter 3 An Alternative Distortionless High-resolution DoA Estimation Method

In DoA estimation, more a priori information and computation usually lead to better performance. The MVDR algorithm requires computation of the inverse of the data covariance matrix. Hence it performs better than the Delay-and-Sum method. The MUSIC algorithm requires eigen-decomposition and the number of signal sources to perform subspace segmentation. Hence the MUSIC algorithm has superior resolution even dealing with closely-situated sources comparing to the MVDR algorithm.

However, the MUSIC algorithm is not a distortionless algorithm in terms of reflecting the true amplitude of the signal of interest. Inspired by the linkage between MVDR and MUSIC, an alternative distortionless DoA estimation method is proposed in this chapter. The purpose of this algorithm is to deliver a similar high-resolution result as the MUSIC does while still caps the beam peak to the real amplitude of the signal of interest.

3.1 Formulation

In Section 2.4, the relation between the MVDR and MUSIC algorithms is revealed by manipulating the data covariance matrix. The performance of the MUSIC algorithm is equivalent to the MVDR algorithm dealing with an inverse covariance matrix whose signal subspace is nulled. The idea of this alternative algorithm is to keep the signal subspace unchanged for distortionless property but nulls the noise subspace for higher resolution.

Recall the model of the autocorrelation matrix of the signal from Section 2.2 equation (2.2.9)

$$\mathbf{R} = \mathbf{S}\mathbf{R}_s\mathbf{S}^H + \sigma_n^2\mathbf{I}. \tag{2.2.9}$$

The noise subspace is removed by setting $\sigma_n^2 = 0$. According to equations (2.2.16) and (2.2.13). The reformulated autocorrelation matrix $\widehat{\mathbf{R}}$ is

$$\widehat{\mathbf{R}} = \sum_{\boldsymbol{m=0}}^{\boldsymbol{K-1}} (\lambda_m - \sigma_n^2)\boldsymbol{\beta}_m\boldsymbol{\beta}_m^H = \mathbf{E}_s(\boldsymbol{\Lambda_s} - \sigma_n^2)\mathbf{E}_s^H \,. \tag{3.1.1}$$

Defining the eigenvalue decomposition of $\widehat{\mathbf{R}}$ as:

$$\widehat{\mathbf{R}} = \mathbf{Z}\boldsymbol{\Sigma}\mathbf{Z}^H \tag{3.1.2}$$

where $\boldsymbol{\Sigma}$ is the eigenvalue matrix of $\widehat{\mathbf{R}}$ and:

$$\boldsymbol{\Sigma} = \begin{bmatrix} \boldsymbol{\Lambda}_{alt} & \mathbf{0} \\ \mathbf{0} & \mathbf{0} \end{bmatrix} \tag{3.1.3}$$

$$\boldsymbol{\Lambda}_{alt} = \mathrm{diag}[\lambda_0 - \sigma_n^2, \lambda_1 - \sigma_n^2, \cdots, \lambda_{K-1} - \sigma_n^2] \,. \tag{3.1.4}$$

$\mathbf{Z}$ is the eigenvector matrix of $\widehat{\mathbf{R}}$:

$$\mathbf{Z} = [\mathbf{Z}_s, \mathbf{Z}_n] \tag{3.1.5}$$

where $\mathbf{Z}_s$ has the first K eigenvectors of $\mathbf{Z}$ and $\mathbf{Z}_n$ keeps the rest of M-K eigenvectors.

The optimization problem is proposed based on the MVDR principle as:

$$\min_{\mathbf{w}} \ \mathbf{w}^H\widehat{\mathbf{R}}\mathbf{w} \tag{3.1.6}$$

$$s.t\ \mathbf{w}^H\mathbf{s}_\theta = 1 \,. \tag{3.1.7}$$

However, this optimization problem could not be solved by applying the Lagrange multiplier method to yield:

$$\mathbf{w}_{opt} = \frac{\widehat{\mathbf{R}}^{-1}\mathbf{s}_\theta}{\mathbf{s}_\theta^H\widehat{\mathbf{R}}^{-1}\mathbf{s}_\theta} \,. \tag{3.1.8}$$

Because, $\widehat{\mathbf{R}}$ is not invertible. Knowing that:

$$\widehat{\mathbf{R}}^{-1} = \mathbf{Z}\boldsymbol{\Sigma}^{-1}\mathbf{Z}^{H} \tag{3.1.9}$$

and:

$$\boldsymbol{\Sigma}^{-1} = \begin{bmatrix} \frac{\mathbf{1}}{\boldsymbol{\Lambda}_{alt}} & \mathbf{0} \\ \mathbf{0} & \frac{\mathbf{1}}{\mathbf{0}} \end{bmatrix}. \tag{3.1.10}$$

One over zero is an expression with no meaning.

If the term $\widehat{\mathbf{R}}^{-1}$could be replaced by the pseudo inverse of $\widehat{\mathbf{R}}$, denoted as $\widehat{\mathbf{R}}^{+}$, the direction-finding function is a similar copy of equation (2.3.21):

$$DF_{Alternative} = \frac{1}{\mathbf{s}_{\theta}^{H}\widehat{\mathbf{R}}^{+}\mathbf{s}_{\theta}}. \tag{3.1.11}$$

This 'natural' extension however does not lead to a correct solution. The following Figure 3.1 shows a numerical test using direction finding function above. In this demonstration test, three unity-power uncorrelated sources located at 30, 40 and 90 degrees with respect to array axis. Input SNR is 5dB. The number of snapshots taken for the covariance matrix is 100.

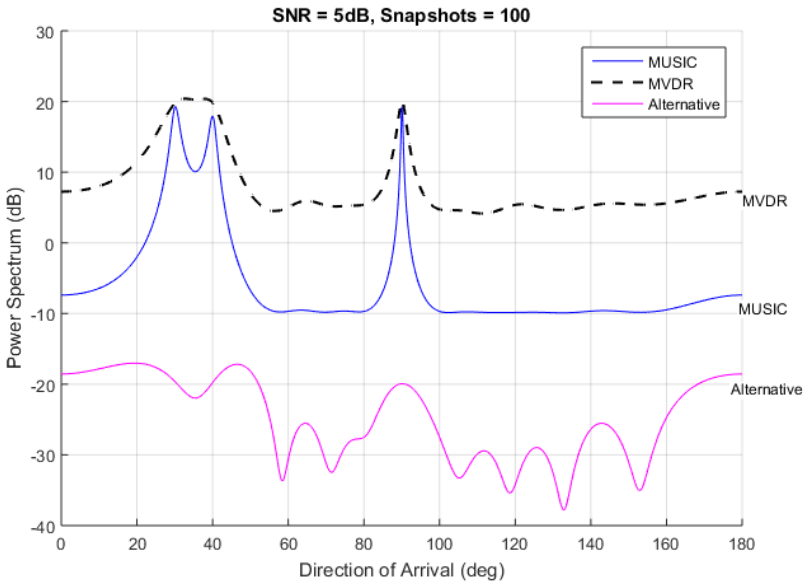

Figure 3.1: Spatial Spectrum of the Proposed Algorithm with Pseudo Inverse Covariance Matrix

It is clear to observe that the result is far from super-resolution, not even close to MVDR. In fact, the spectra plot obtained is erroneous. The reason is explained in the next section.

3.2 Solution of Proposed Algorithm

Instead of using pseudo inverse directly, the optimization problem could also be rewritten as

$$\min_{\mathbf{w}} \ \mathbf{w}^H \mathbf{Z}\boldsymbol{\Sigma}\mathbf{Z}^H \mathbf{w} \tag{3.2.12}$$

$$s.t\ \mathbf{w}^H \mathbf{s}_\theta = 1\,. \tag{3.2.13}$$

Defining

$$\mathbf{Y} = \mathbf{Z}^H \mathbf{w} = \begin{bmatrix} \mathbf{Z}_s{}^H \mathbf{w} \\ \mathbf{Z}_n{}^H \mathbf{w} \end{bmatrix} = \begin{bmatrix} \mathbf{Y}_s \\ \mathbf{Y}_n \end{bmatrix} \tag{3.2.14}$$

$$\mathbf{w} = \mathbf{Z}\mathbf{Y} \tag{3.2.15}$$

The problem now is

$$\min_{\mathbf{Y}} \ \mathbf{Y}^H \mathbf{\Sigma} \mathbf{Y} \tag{3.2.16}$$

$$s.t\ (\mathbf{ZY})^H \mathbf{s}_\theta = 1. \tag{3.2.17}$$

By applying equations (3.1.3), (3.1.5) and (3.2.14), the problem could be rewritten into:

$$\min_{\mathbf{Y}_s} \ \mathbf{Y}_s{}^H \ \mathbf{\Lambda}_{alt} \mathbf{Y}_s \tag{3.2.18}$$

$$s.t\ (\mathbf{Z}_s \mathbf{Y}_s + \mathbf{Z}_n \mathbf{Y}_n)^H \mathbf{s}_\theta = 1\ . \tag{3.2.19}$$

The $\mathbf{Y}_s$ could be solved by applying the Lagrange multiplier method to this reformed problem:

Defining the Lagrange function as:

$$L(\mathbf{Y}_s, \lambda) = \mathbf{Y}_s{}^H \ \mathbf{\Lambda}_{alt} \mathbf{Y}_s + \lambda((\mathbf{Z}_s \mathbf{Y}_s + \mathbf{Z}_n \mathbf{Y}_n)^H \mathbf{s}_\theta - 1)\ . \tag{3.2.20}$$

The gradients are:

$$\frac{\partial L}{\partial \mathbf{Y}_s} = \mathbf{\Lambda}_{alt} \mathbf{Y}_s + \lambda \mathbf{Z}_s{}^H \mathbf{s}_\theta = \mathbf{0} \tag{3.2.21}$$

$$\frac{\partial L}{\partial \lambda} = (\mathbf{Z}_s \mathbf{Y}_s + \mathbf{Z}_n \mathbf{Y}_n)^H \mathbf{s}_\theta - 1 = \mathbf{0}\ . \tag{3.2.22}$$

The solution of $\mathbf{Y}_s$ could be derived as fellows:

$$\mathbf{Y}_s = \mathbf{\Lambda}_{alt}^{-1} \mathbf{Z}_s^H \mathbf{s}_\theta \left(\mathbf{s}_\theta^H \mathbf{Z}_s \ \mathbf{\Lambda}_{alt}^{-1} \mathbf{Z}_s^H \mathbf{s}_\theta\right)^{-1} (1 - (\mathbf{Z}_n \mathbf{Y}_n)^H \mathbf{s}_\theta)\ . \tag{3.2.23}$$

Now the output power of array which is also the direction-finding function is

$$P = \mathbf{Y}_s{}^H \ \mathbf{\Lambda}_{alt} \mathbf{Y}_s = \left(\mathbf{s}_\theta^H \mathbf{Z}_s \ \mathbf{\Lambda}_{alt}^{-1} \mathbf{Z}_s^H \mathbf{s}_\theta\right)^{-1} (1 - (\mathbf{Z}_n \mathbf{Y}_n)^H \mathbf{s}_\theta)^2\ . \tag{3.2.24}$$

Defining

$$P_0 = \left(\mathbf{s}_\theta^H \mathbf{Z}_s \, \mathbf{\Lambda}_{alt}^{-1} \mathbf{Z}_s^H \mathbf{s}_\theta\right)^{-1} = \frac{1}{\mathbf{s}_\theta^H \widehat{\mathbf{R}}^+ \mathbf{s}_\theta} \, . \tag{3.2.25}$$

Comparing equation (3.2.24) with (3.1.11), it is obvious that two equations share a common term P_0, but (3.2.24) has an extra scaling term as follows:

$$P = \mathbf{Y}_s{}^H \, \mathbf{\Lambda}_{alt} \mathbf{Y}_s = P_0 (1 - (\mathbf{Z}_n \mathbf{Y}_n)^H \mathbf{s}_\theta)^2 \, . \tag{3.2.26}$$

Missing scaling term $(1 - (\mathbf{Z}_n \mathbf{Y}_n)^H \mathbf{s}_\theta)^2$ is the reason why Figure 3.1 shows a poor result. Noted that only at the true source directions, the inner product between steering vector $\mathbf{s}_\theta$ and noise subspace $\mathbf{Z}_n$ is zero, so that $(\mathbf{Z}_n \mathbf{Y}_n)^H \mathbf{s}_\theta$ equals to zero and P equals to P_0. The final spectrum is non-negative and equals to the true signal power P_0 times a scaling term. The scaling term has to be a value no smaller than 0 and no larger than 1, which means the term $(\mathbf{Z}_n \mathbf{Y}_n)^H \mathbf{s}_\theta$ is also value from 0 to 1.

3.3 Computer Simulation

A computer simulation is set to test the performance of direction finding function (3.2.24). A 10-element ULA is used. There are 3 unity-power narrowband sources coming from 30, 40 and 90 degrees with respect to the array axis. The input SNR is 10 dB. 100 snapshots are taken to form the covariance matrix. The simulation result for method proposed in the last section is shown in Figure 3.2.

Compared with Figure 3.1, which is the result of using pseudo inverse covariance matrix, the result from equation (3.2.24) in Figure 2 is clearer and with a higher output SNR.

This algorithm still faces the issue of stability. An example of unstable plot is shown in Figure 3.3. A simple moving average filter is good enough to remove those sudden clips in the spectrum. Figure 3.2 is a plot after filter smoothing.

The algorithm stability is related to the snapshot taken and input SNR. The covariance matrix is closer to ideal with he longer snapshot taken and higher input SNR. Ill-condition signal covariance matrix is the cause of the unstableness.

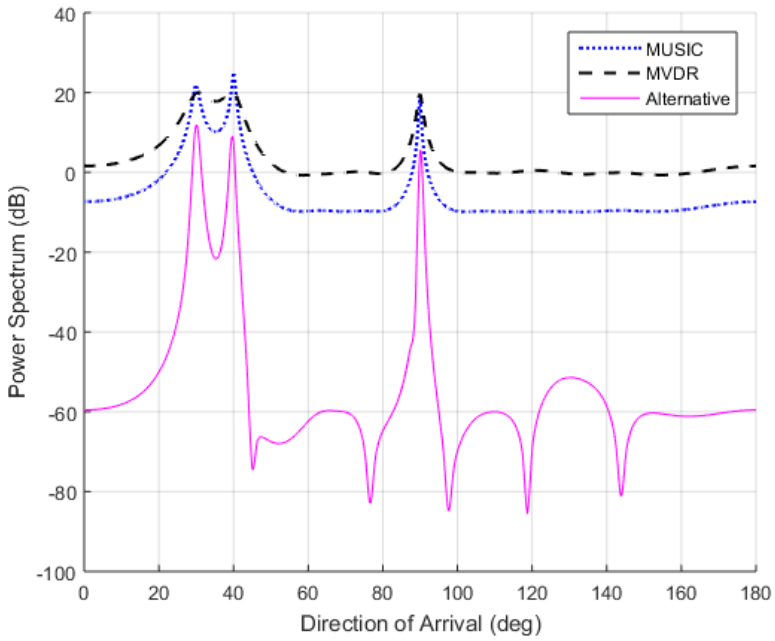

Figure 3.2: Spatial Spectrum of the Proposed Algorithm

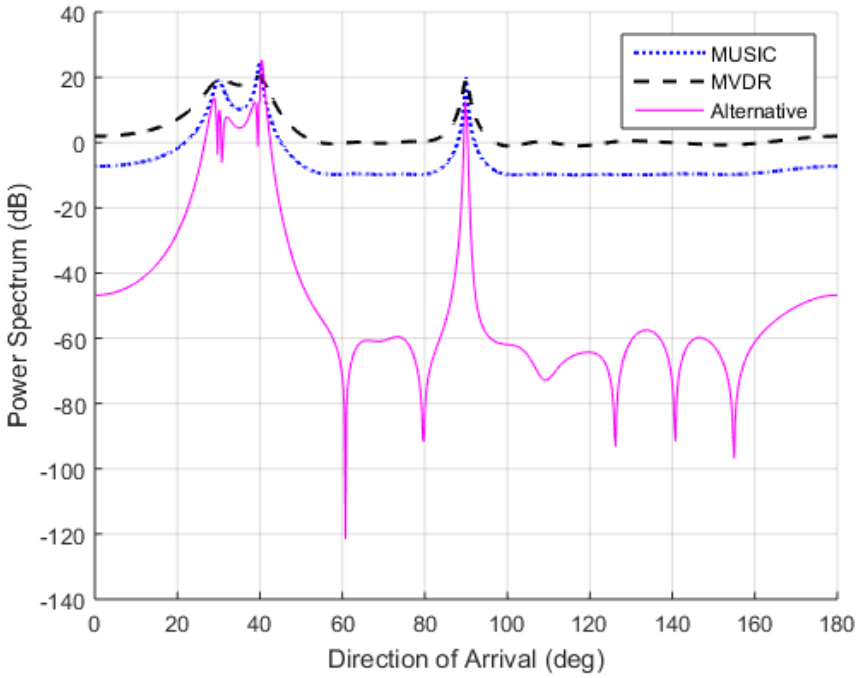

Figure 3.3: Unstable Result of Alternative Super-resolution Algorithm

3.4 Summary

An alternative high-resolution algorithm is proposed in this chapter. Inspired by the relationship between the MVDR and the MUSIC algorithm, the proposed algorithm applies the idea of imposing negative infinity power of noise into the signal covariance matrix of the MVDR algorithm. Since the signal power remains unattended, the ideal spectrum should reflect the true signal power which the MUSIC algorithm does not.

Computer simulation with 3-source ULA scenario delivers promising result when the input SNR is high enough (above 10 dB). As the input SNR decreases, the performance starts to be unstable with odd clip at signal peak. By applying the moving average filter to the spectrum could reduce the clip.

Chapter 4 Improved Scanning Method for the MUSIC Algorithm

In Chapter 3, an alternative algorithm is proposed based on the study of the mathematical nature of the MUSIC algorithm. In this chapter, an improved scanning method would be introduced and studied to reduce the computational complexity of the MUSIC algorithm based on its spectrum nature.

4.1 Observation and Notation

For the conventional MUSIC algorithm introduced in Chapter 2, the spatial spectrum is usually plotted such as that in Figure 4.1.

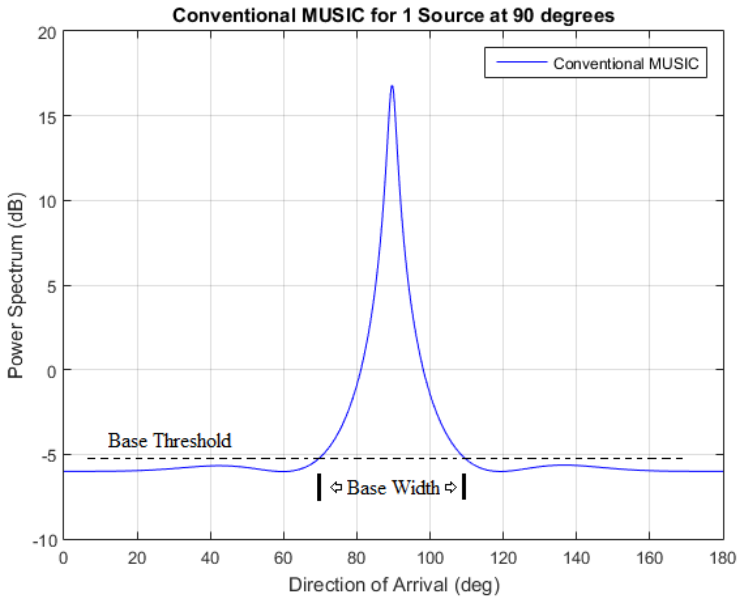

Figure 4.1: Spatial Spectrum of the Conventional MUSIC Algorithm (1-source)

The source direction always appears as a cusp-shape peak. Two parameters are introduced to describe the peak more specifically, base width and base threshold. Base width describes the size of range where the peak appears. Base threshold is associated with the quiescent pseudo noise level. After finishing numerous MUSIC algorithm simulations, an interesting fact is found. When the source direction is confirmed, the base width and base threshold is only affected by the number of array elements, regardless of the input SNR or the number of snapshots taken. The base width and base threshold will decrease proportionally while the number of array elements increases and vice-versa.

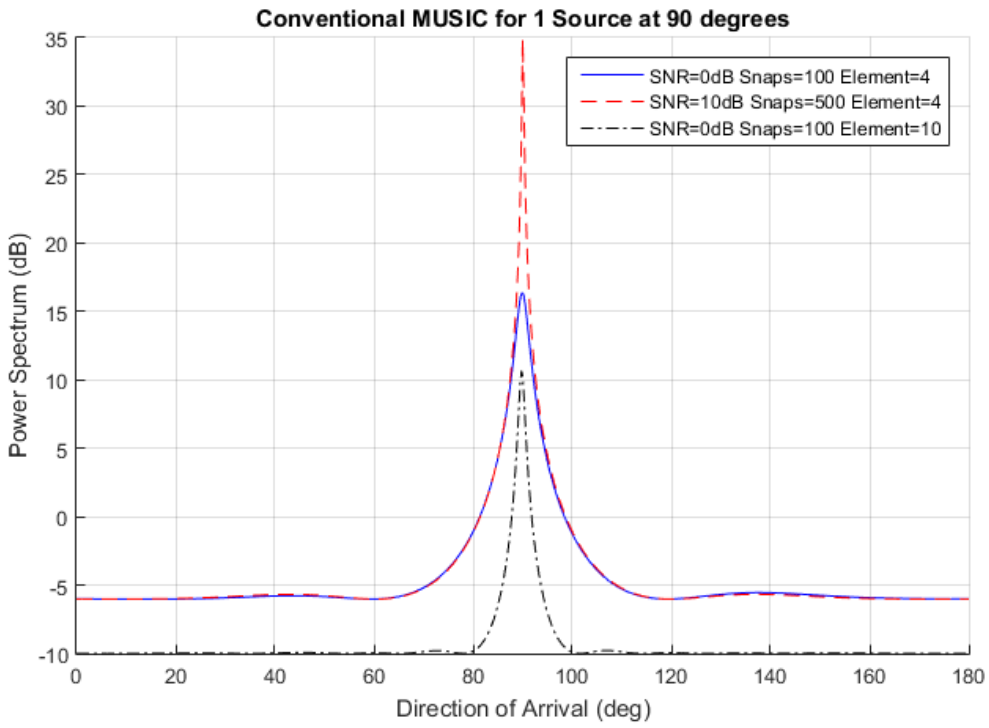

Figure 4.2: The MUSIC Spatial Spectrum for different Array Sizes (1-source)

Figure 4.2 shows the MUSIC spectrum in 3 different cases which proves this fact. For solid blue and red dash spectrum the SNR and snapshot are both different, yet the base widths and base thresholds are identical.

This fact narrows the directional range of interest only based on a common knowledge, the number of array elements. Hence the computational load of the MUSIC beamforming could be reduced by using an improved scanning method.

The idea of improved scanning method is to scan the entire FoV roughly based on the estimation of base width. The rough range of interest would be located with the help of estimated base threshold and followed by fine-resolution scan in those ranges. The total number of scans will be lesser, and the overall computational load is reduced.

4.2 Formulation

The exact relations among base width, base threshold and the number of array elements must be studied in order to perform the improved scanning method.

Uniform linear array is used to capture only 1 signal coming from 90 degrees with respect to the array front in 0dB SNR. The number of snapshots is 100. It is important to know that when signal is coming from small angles like 10 or 20 degrees with respect to the array front, the base width might have a larger range. In case any potential base width is missed, it will be studied as narrow as possible. The smallest base width generally appears in 90 degrees scenario.

The cusp-shape peak represents a dramatical change in the spectrum amplitude. Hence the base width is found when the difference between two adjacent spectrum values is over 0.1 dB.

For number of elements bearing from 2 to 20, the base width is shown in Table 4.1:

Elements Number	Base Width (degree)									
2-11	37.75	33	29.25	25.75	23.25	21	19	17.25	16	15.25
12-20	14.25	13.25	12.5	11.75	11.25	10.75	10	9.5	9.25	-

Table 4.1: Base Width Data w.r.t Array Size

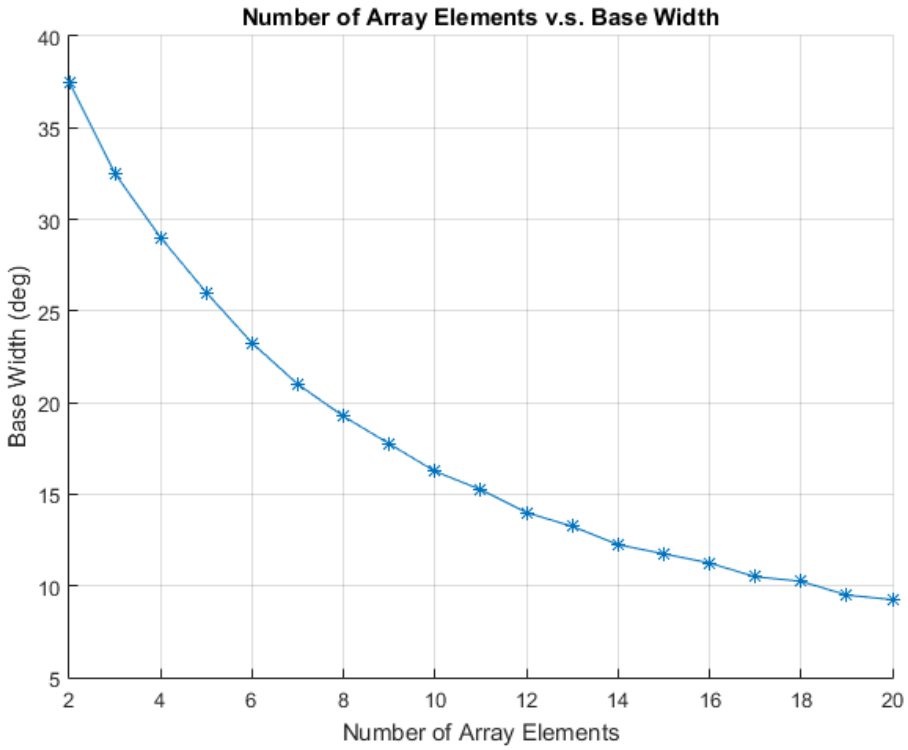

Figure 4.3: Base Width vs. Array Size for the MUSIC Algorithm (1-source at 90 degrees)

From the plotted graph in Figure 4.3, a mathematical relation between number of array elements and base width could be estimated as the following equation:

$$BaseWidth = \exp(0.0027 * M^2 - 0.1304 * M + 3.8207) \qquad (4.2.1)$$

where M indicates the number of array elements and the unit of term $BaseWidth$ is degree.

After the base width is determined, it is easy to find base threshold accordingly.

For number of elements varies from 2 to 20. The base width is found accordingly as:

Elements Number	Base Threshold (dB)									
2-11	3.22	-1.23	-3.64	-5.32	-6.52	-7.46	-8.24	-8.92	-9.44	-9.90
12-20	-10.38	-10.81	-11.11	-11.44	-11.81	-12.09	-12.31	-12.53	-12.76	

Table 4.2: Base Threshold Data w.r.t Array Size

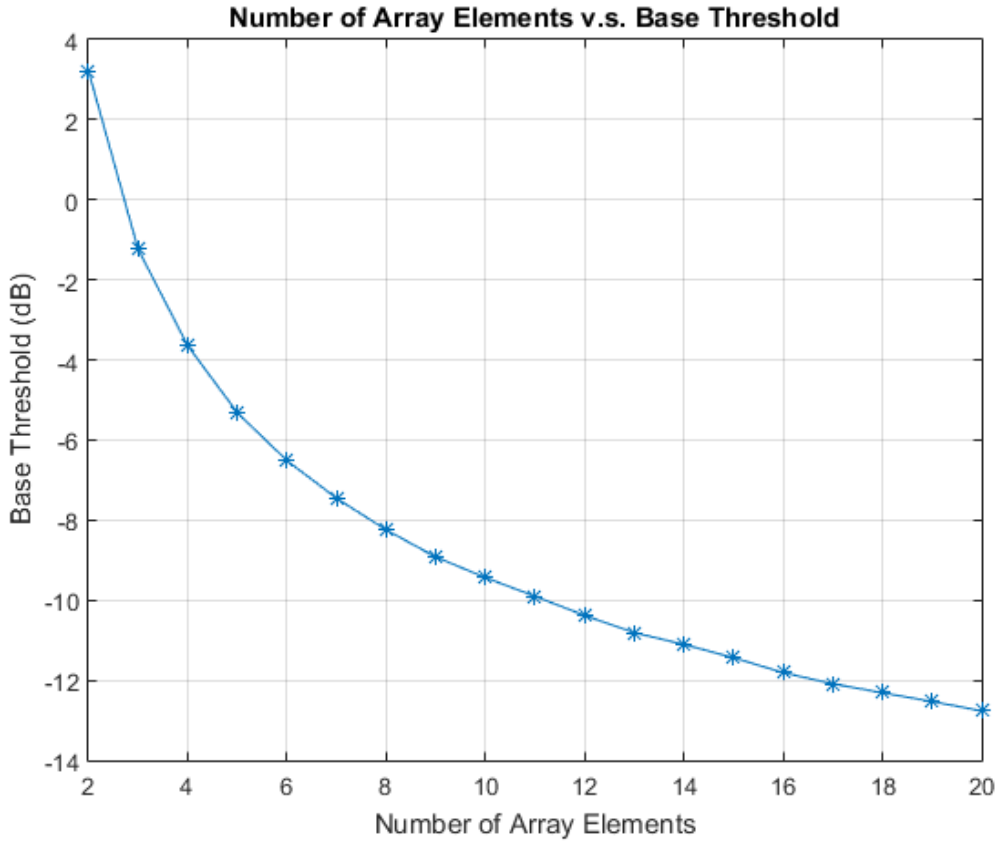

Figure 4.3: Base Threshold vs. Array Size for the MUSIC Algorithm (1-source at 90 degrees)

Theoretically, the base threshold (dB) could be calculated as:

$$BaseThreshold = 10 * \log_{10}\left(\frac{1}{M}\right). \quad (4.2.2)$$

However in practice, the relationship between number of element and base threshold could not be described perfectly in one equation, since the base threshold may rise for multiple-source cases. For the cases with array size below 10, equation (4.2.3) matches the plot in Figure 4.3. For the case with size between 10 and 17, equation (4.2.4) would be used for base threshold estimation.

$$BaseThreshold = \exp(-0.0067 * M^2 + 0.2010 * M + 0.9112 + 3.1416i), \quad (4.2.3)$$

$$BaseThreshold = -\exp(0.0353 * M + 1.8920). \quad (4.2.4)$$

It is also important to note that lower estimated base threshold only causes less computational efficiency but not a miss or fault estimation.

4.3 Scanning Method and Simulation

The aim of this improved scanning method is to reduce the number of total scans without losing any precision. Firstly, the entire FoV is scanned in a large scan step size in order to find potential cusp-shape peak. Since the full range of the cusp-shape peak is equal to base width, the rough scan step size should be no larger than half of the base width in order to meet the Nyquist criterion. Secondly, the significant spectrum samples are selected by filtering out all the spectrum value below the base threshold, which also neglects the directions that is covered by noise only. The potential peak now lies within the remaining range. Finally, refine scanning is performed between two directional adjacent (according to the rough scan step size) significant spectrum samples. The step size of refine scanning is much smaller in order to reveal the distinct signal direction. If two sequential significant samples are not directional adjacent, there must be more than one potential peak hidden. The refined scanning procedure will skip the direction range between those two significant samples and continue refine the rest. The scanning algorithm descried is shown in Figure 4.4.

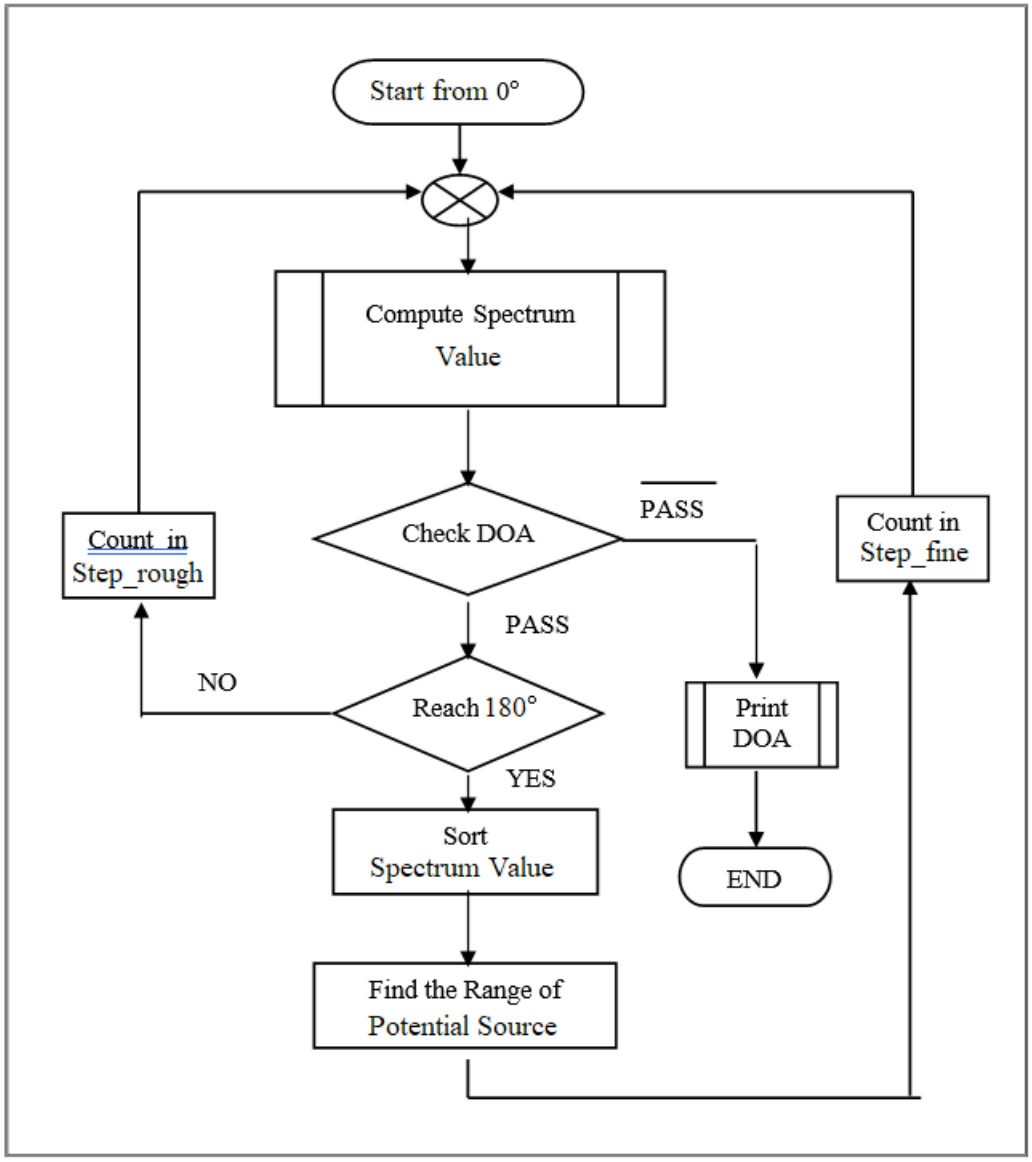

Figure 4.4: Flow Chart for the Improved Scanning Method

1-sourse simulation is performed with an 8-element ULA. SNR equals to 0 dB. Number of snapshots is 100. The signal direction is 40 degrees with respect to the array front. Rough scan step size is chosen to be half of the base width and the refine step size is 0.25 degree.

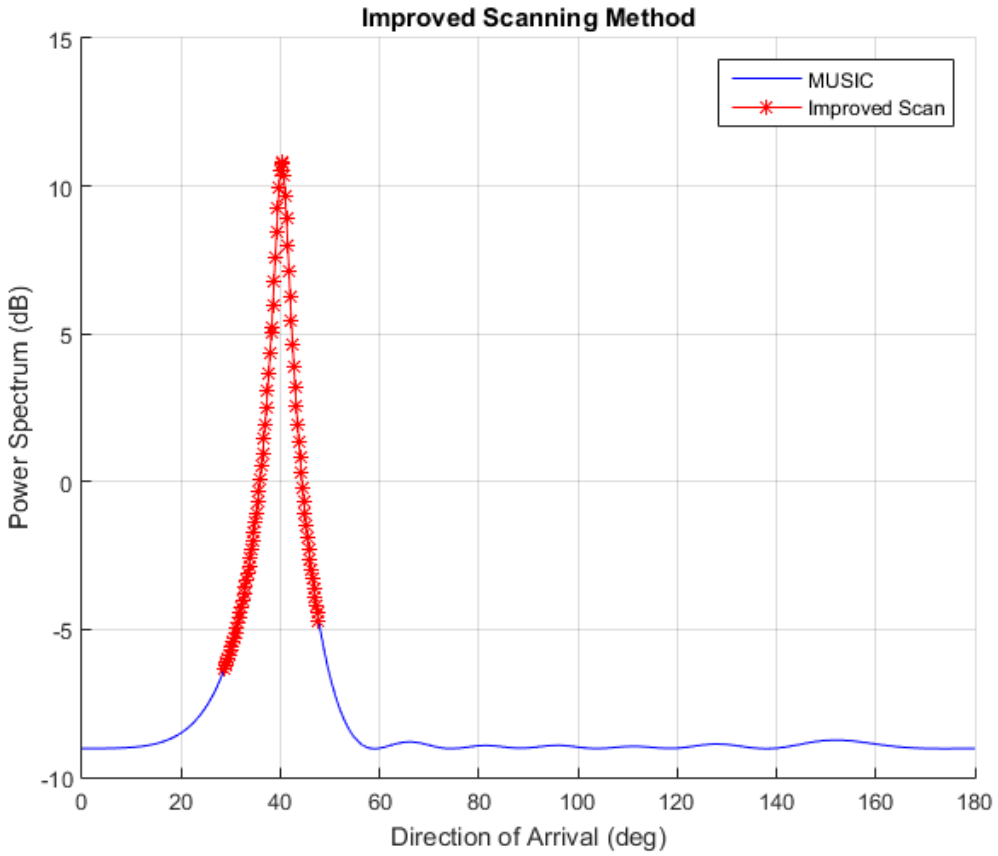

Figure 4.5: MUSIC Spectrum with Improved Scanning Method (1-source)

The cross dots represent the spectrum delivered by improved scanning method. The total sample number is much less the conventional spectrum, which means less scanning is made yet the signal direction peak is revealed precisely.

The same result shows in multiple sources simulations. 3 sources emit from 30, 40 and 120 degrees and captured by 15-element ULA. SNR equals to 0 dB. Number of snapshots is 100. Rough scan step size is chosen to be half of the base width and the refine step size is 0.25 degree.

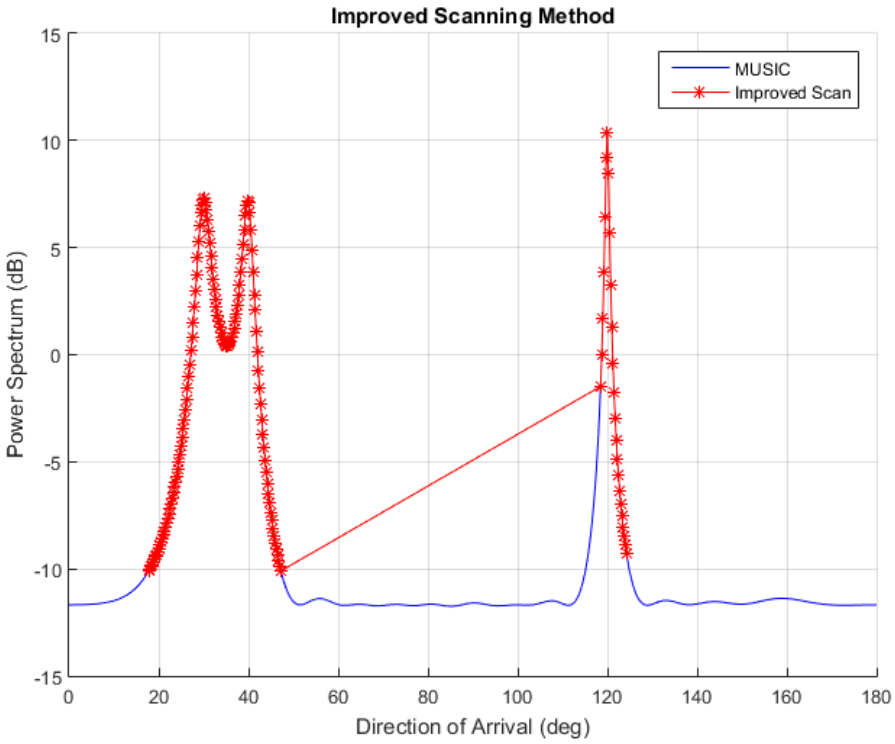

Figure 4.6: MUSIC Spectrum with Improved Scanning Method (3-source)

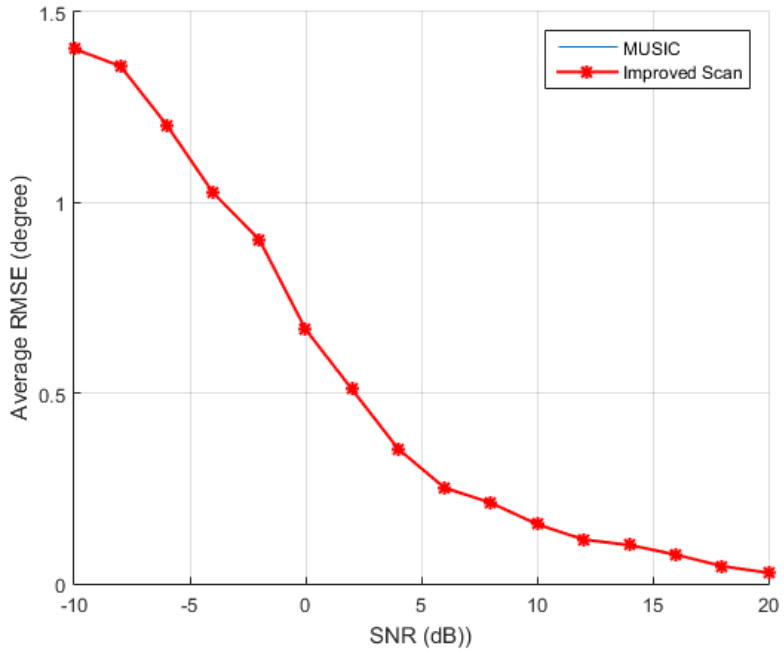

Figure 4.7: RMSE Comparison for the MUSIC and Improved Scanning Method (3-source)

The straight line linking 40 and 120 degrees is because of the default plot mechanism of the Matlab software. There is no cross dot on that line, which means there is actually no data and no computation involved. The result is as efficient as the 1-source scenario. No extra scans happen in the noise range.

The average root-mean-square error (RMSE) of the DoA estimation is a parameter that measure the estimation accuracy, which would be introduced in detail in next chapter. Two lines (solid and dotted) are identical which means the improved scanning method does not lose any resolution capability with respect to the MUSIC algorithm using conventional scanning method.

4.4 Evaluation

According to the notation definition in Chapter 2, K represents the number of uncorrelated narrowband signal sources to be detected, M indicates the number of sensors in the array and N as the number of direction scans across the entire FoV.

The load to compute a proper eigenvalue decomposition is $O(M^3)$. This is a procedure happened before the scan and the cost is the same for both the conventional MUSIC and the MUSIC applied improved scanning method. The improved scanning method requires three extra one-time computation for base threshold, base width and rough scan step accordingly. The cost is $O(7)$. The computational load for calculating signal spectrum value in each scan is $O((M-K+1)M^2+M)$.

Hence the total computational load for conventional MUSIC algorithm is $O(M^3+(M-K+1)M^2N+MN)$ and for the improved scanning method is $O(M^3+(M-K+1)M^2N_{reduce}+MN_{reduce}+7)$. The total scan number for improved scanning method N_{reduce} will be counted in the simulations.

For the 1-source simulation done in last part, 8-element array is used. The fine scan step used for conventional and improved method is 0.25 degrees. The conventional MUSIC method did 721 scans in total. However, for the improved scanning method the rough scan is performed only 19 times and 78 times for the fine scan. The total computational loads are $37.5 * 10^4$ and $5.1 * 10^4$. The overall computational complexity is reduced by 86.4%.

For the 3-source simulation, 15-element ULA is implemented. The fine scan step remains the same, which means the total scan number for the conventional method remains 721. The rough and fine scan numbers for the improved scanning method is now 31 and 144. The total computational loads are $212.3 * 10^4$ and $51.8 * 10^4$. The overall computational complexity is reduced by 75.6%.

The following figure shows the computational load reduction performance with respect to the number of array element used. The samples are taken in 3-source scenarios.

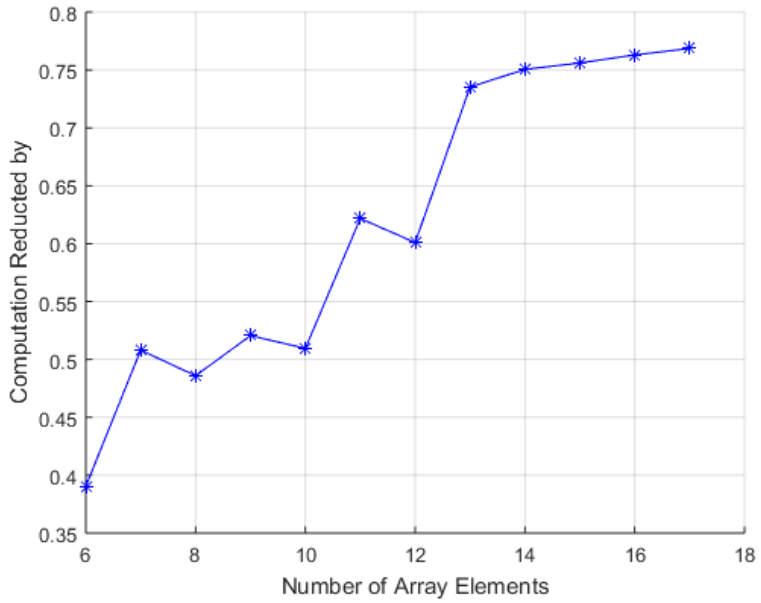

Figure 4.8: Computation Reduction vs. Array Size (3-source)

From Figure 4.6, one could know that generally speaking the computation reduction rate increases when the size of array grows larger.

The improved scanning method proposed in this chapter is an effective method to reduce computational load for the MUSIC beamforming algorithm. It is based on the spectrum nature of the MUSIC algorithm. This method introduces two parameters, base width and base threshold, to quantize the beam nature. These two parameters are independent from signal environment and only linked to the size of array. With proper base width and threshold settings, the computational complexity of the MUSIC algorithm could be reduced more than 50%.

4.5 Summary

In this chapter, a scanning method is introduced to reduce the computational load for the MUSIC algorithm. The new scanning method is proposed based on the nature of the spectrum of the MUSIC algorithm. Two parameters, base width and base threshold are defined to quantify the relationship between the cusp-shape peak of the spatial spectrum and the number sensors. They are inversely proportional to the number of element only. With the help of these two parameters, an improved 2-step scan is performed to the MUSIC algorithm. By dividing the scanning process into two relatively faster scanning periods, the computational load is reduced significantly with no loss of resolution in the computer simulation.

These is still a problem remained. The numerical expression of the relationship derived in this chapter has an element limitation of 20. For an array with element more than 20, a new expression should be calculated. A more generalized expression is yet to be found.

Chapter 5 UR-Like DoA Estimation Without Estimating the Number of Sources

In many DoA estimation application scenarios, the explicit number of sources is not available in advance. The high-resolution eigen-structure based algorithms like the MUISC and UR all require exact determination of effective rank of the covariance data matrix, which is associated with the number of sources. There are serval algorithms designed to estimate the effective rank of a matrix, like Akaike Information Criterion (AIC) and Minimum Description Length (MDL) [12]. However, these algorithms may deliver wrong estimation of the rank with small sample sizes and low input SNR. The MVDR method as a conventional solution does not require number of sources as input. Its limitations are addressed in Chapter 2.3.1.

In this chapter, a new optimization problem is proposed. This new algorithm tries to deliver a high-resolution spectra plot without the number of sources.

5.1 Formulation

In the formulation of the MVDR algorithm, the constraint is linear as shown in equation (2.3.19). Replace the linear constraint with a quadratic one borrowed from the objective function from the UR algorithm, equation (2.3.28). Compare the linear, quadratic constraint focuses only on the power and the phase information is ignored.

The proposed optimization problem is:

$$\min_{\mathbf{w}} \ \mathbf{w}^H \mathbf{R} \mathbf{w} \tag{5.1.1}$$

$$s.t\ \frac{1}{\Delta\theta}\int ||\mathbf{w}^H\mathbf{s}_\theta - \mathbf{1}||^2\, \boldsymbol{d\theta} = c \tag{5.1.2}$$

where *c* represents a positive constant.

Expanding the integration in constraint equation, we have:

$$\min_{\mathbf{w}}\ \mathbf{w}^H\mathbf{R}\mathbf{w} \tag{5.1.3}$$

$$s.t\ \mathbf{w}^H\mathbf{Q}\mathbf{w} - \mathbf{w}^H\mathbf{P} - \mathbf{P}^H\mathbf{w} + \mathbf{1} = c \tag{5.1.4}$$

where

$$\mathbf{Q} = \frac{1}{\Delta\theta}\int \mathbf{s}_\theta\mathbf{s}_\theta^H\, \boldsymbol{d\theta} \tag{5.1.5}$$

$$\mathbf{P} = \frac{1}{\Delta\theta}\int \mathbf{s}_\theta\, \boldsymbol{d\theta}\ . \tag{5.1.6}$$

Apply the Lagrange multiplier method to this problem and define the Lagrange function as:

$$L(\mathbf{w},\lambda) = \mathbf{w}^H\mathbf{R}\mathbf{w} + \lambda(\mathbf{w}^H\mathbf{Q}\mathbf{w} - \mathbf{w}^H\mathbf{P} - \mathbf{P}^H\mathbf{w} - c)\ . \tag{5.1.7}$$

The gradient with respect to weight vector is:

$$\frac{\partial L}{\partial \mathbf{w}} = \mathbf{R}\mathbf{w} + \lambda(\mathbf{Q}\mathbf{w} - 2\mathbf{P}) = \mathbf{0}\ . \tag{5.1.8}$$

Because of the term $2\mathbf{P}$, the equation cannot be rewritten into $(\mathbf{R} + \lambda\mathbf{I})\mathbf{w} = \mathbf{0}$ form for Generalized Eigenvalue Solution like the MUSIC-Like algorithm. To avoid the trouble caused by this quadratic hard constraint, penalty function approach is chosen for a close approximation.

5.2 Penalty Function Solution

The optimization problem now turns out to be an unconstrained minimization problem:

$$\min_{\mathbf{w}} (1-\alpha)\mathbf{w}^H\mathbf{R}\mathbf{w} + \alpha\frac{\mathbf{1}}{\Delta\boldsymbol{\theta}}\int \left|\left|\mathbf{w}^H\mathbf{s}_\theta - \mathbf{1}\right|\right|^2 \boldsymbol{d}\theta \tag{5.2.9}$$

where α is the penalty coefficient.

By setting the gradient with respect to weigh vector to zero:

$$\frac{\partial F}{\partial \mathbf{w}} = (1-\alpha)\mathbf{R}\mathbf{w} + \alpha(\mathbf{Q}\mathbf{w} - 2\mathbf{P}) = \mathbf{0}, \tag{5.2.10}$$

solution is obtained as:

$$\mathbf{w}_{penalty} = \left((1-\alpha)\mathbf{R} + \alpha\mathbf{Q}\right)^{-1}\alpha\,\mathbf{P}\,. \tag{5.2.11}$$

The direction-finding function is the array response which could be expressed as

$$DF_{URLike\_penalty} = |\mathbf{w}_{penalty}^H\mathbf{s}(\theta)| = \left(\left((1-\alpha)\mathbf{R} + \alpha\mathbf{Q}\right)^{-1}\alpha\,\mathbf{P}\right)^H\mathbf{s}(\theta)\,. \tag{5.2.12}$$

5.3 Simulation and Performance Evaluation

5.3.1 Computer Simulation

A computer simulation is made based on equations (5.2.11) and (5.2.12). The array used is a 10-element ULA. The uncorrelated unity power point sources locate at 30, 40 and 90 degrees with respect to the reference array axis. SNR equals to 5dB and 100 snapshots are taken to form the covariance matrix. The value of alpha is set to be 0.2. The influence of alpha will be discussed later. $\Delta\theta$ is equal to 0.25 degree.

The simulation result shown in Figure 5.1 shows that the proposed method is possible to achieve a high-resolution estimation similar to the MUSIC or UR algorithms without the number of sources information. Because the spectrum of the proposed algorithm is similar to the UR algorithm, the proposed algorithm is named as the UR-Like algorithm.

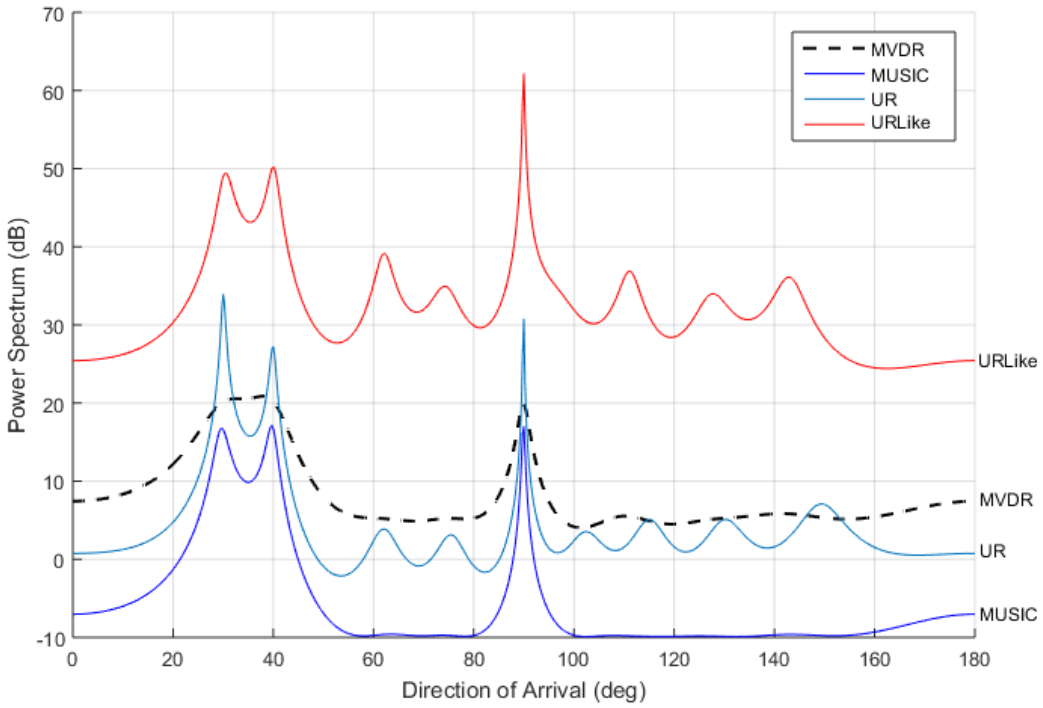

Figure 5.1: The UR-Like Penalty Solution Result with Fixed Alpha=0.2

5.3.2 Performance Evaluation

Two parameters are measured to study the performance of the proposed algorithm, probability of successful estimation and root-mean-squared error (RMSE) of a successful estimation.

5.3.2.1 Resolution Capability

Considering the simulation environment which contains 3 sources located at 30, 40 and 90 degrees with respect to the array axis. 10-element ULA is used. In this test, the value of alpha is still fixed to 0.2 in the proposed UR-Like algorithm. The capability of resolution is measured by the probability of successful estimation. This probability is studied by taking 200 Monte-Carlo trials against different input SNRs in comparison with the MUSIC and UR algorithms. A successful estimation is considered only when all sources directions are resolved when a significant peak appears in each critical spatial region of DoA. The critical spatial region is defined as:

$$[\theta_i - \Delta\theta, \quad \theta_i + \Delta\theta], \ \ for\ i \in M \tag{5.3.13}$$

where $\Delta\theta$ is the half of minimum source angular difference. In this simulation case, $\Delta\theta = 5$ degrees:

$$\Delta\theta = \frac{\min(\theta_i - \theta_j)}{2}, \quad \forall i,j\ and\ i \neq j \in M\ . \tag{5.3.14}$$

SNR ranges from -20 to +20 dB. Step size is 2 dB.

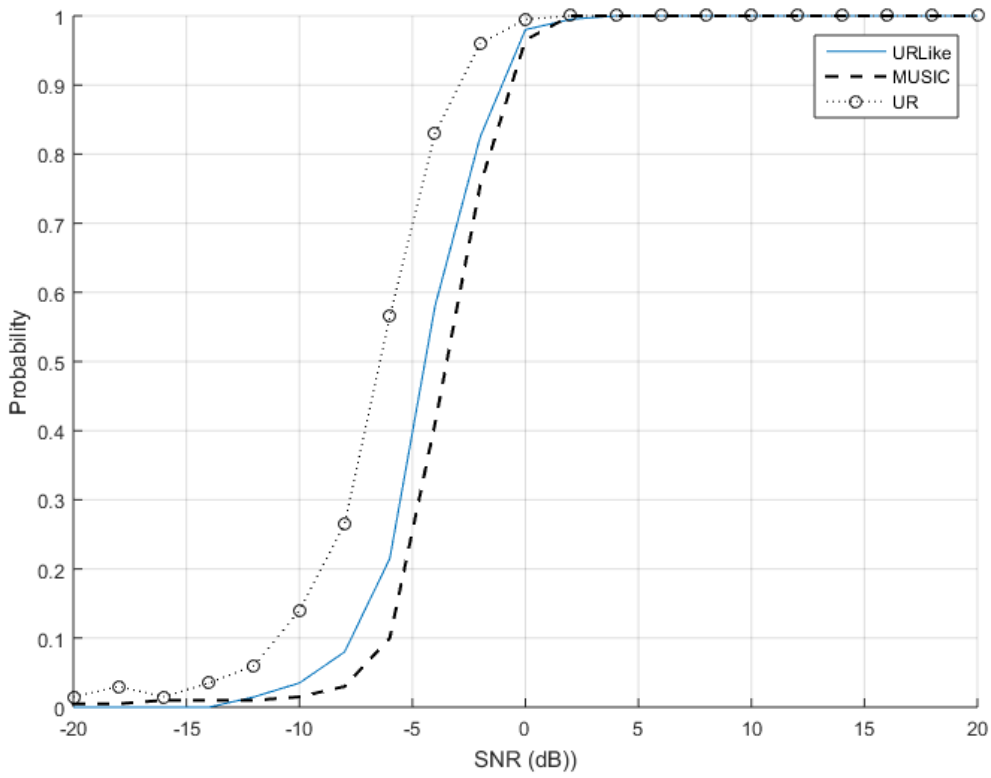

Figure 5.2: Estimation Resolution Probability for the UR-Like, MUISC and UR Algorithms

Among these three high resolution methods, the proposed UR-Like algorithm is a balance between the UR and MUSIC algorithms. The UR method performs the best for low SNR conditions with a higher probability of successful estimation. Without the information of true number of sources, The UR-Like algorithm is not as reliable as the UR but still outperforms the MUSIC.

5.3.2.2 Estimation Accuracy

Following the same setup, the estimation accuracy is measured by the average root-mean-square error (RMSE) of the DoA estimation of all sources against different SNR conditions. RMSE is calculated by:

$$RMSE = \frac{1}{K}\sum_{i=0}^{K-1}\sqrt{\frac{1}{N}\sum_{j=1}^{N}(\hat{\theta}_i - \theta_i)^2} \tag{5.3.15}$$

where N is the number of successful estimations, $\hat{\theta}_i$ is the estimated DoA.

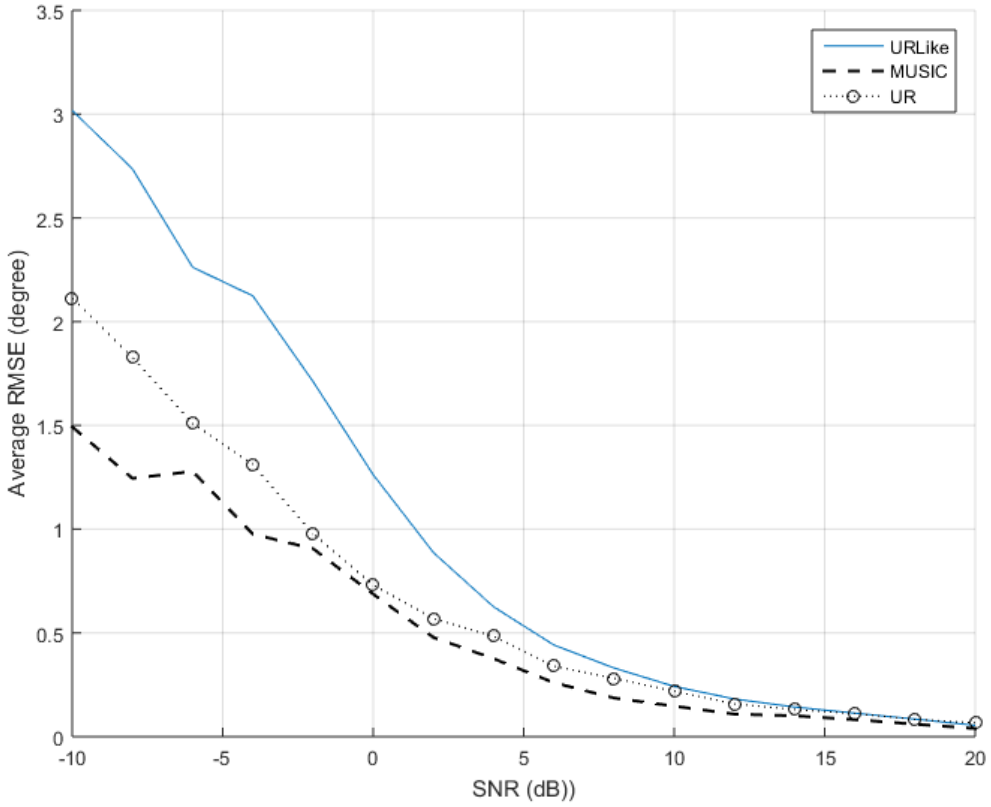

Figure 5.3: RMSE of DoA Estimation Comparison for UR-Like, MUSIC and UR Algorithms

In terms of accuracy of estimation, both UR and UR-Like algorithms are not as good as MUSIC, because of the phase optimization issues of UR. The constraint (5.1.2) is originally written as

$$s.t\ \frac{1}{\Delta\theta}\int \left|\left|\mathbf{w}^H\mathbf{s}_\theta - e^{j\tau(\theta)}\right|\right|^2 \boldsymbol{d\theta} = c \tag{5.3.16}$$

The term $\tau(\theta)$ is a quantity that can be optimized. An averaging method to solve this phase issue is proposed in the literature [10].

The following tables elaborate the RMSE comparison in a more detailed way.

SNR (dB)	DoA (degree)	MUSIC (degree)	UR (degree)	UR-Like (degree)
0	30	1.066	1.196	1.782
	40	0.812	0.811	1.635
	90	0.169	0.243	0.351
10	30	0.246	0.342	0.304
	40	0.178	0.233	0.299
	90	0.031	0.103	0.129
20	30	0.064	0.187	0.085
	40	0.035	0.077	0.066
	90	0	0	0

Table 5.1: RMSE of Estimation with respect to Input SNR at Snapshot = 100

Table 5.1 shows the RMSE test result especially in high SNR scenarios. It is obvious that the RMSE decreases along with the increasing input SNR for all three algorithms. The input SNR influents the phase issue of the UR and the UR-Like algorithm more dramatically comparing to the MUSIC algorithm. In the scenarios where SNR is larger than 10dB, the RMSE of the DoA estimation of the UR-Like algorithm is about 35% more than the MUSIC algorithm, where at -10dB cases the RMSE difference is 200%.

Table 5.2 shows the RMSE performance versus the number of snapshots taken at input SNR equals to 0dB. The number of snapshots taken does affect the value of RMSE of all three algorithms. The larger the number of snapshots taken, the better the performance is. However, the influence is not as great as the input SNR.

Snapshot (frame)	DoA (degree)	MUSIC (degree)	UR (degree)	UR-Like (degree)
50	30	1.142	1.460	1.945
	40	1.163	1.242	1.894
	90	0.232	0.412	0.578
100	30	0.937	1.177	1.667
	40	0.804	0.872	1.382
	90	0.162	0.286	0.390
150	30	0.747	0.878	1.526
	40	0.689	0.734	1.345
	90	0.152	0.232	0.289
200	30	0.658	0.824	1.468
	40	0.500	0.671	1.224
	90	0.135	0.204	0.262

Table 5.2: RMSE of Estimation with respect to Snapshots at SNR = 0dB

5.3.2.3 Influence of Alpha

Another simulation is taken to examine the influence of alpha. The environment setting remains unchanged. The value range of alpha is zero to one. Step size is 0.1.

As alpha approaches to 0, the whole Figure 5.4 moves upwards. Generally speaking, alpha has very minor influence on the output performance. Such a guess can be also proven by testing with probability of successful estimation. The value of alpha is chosen to be 0.0001, 0.2, 0.5 and 0.9 with 4 different SNR scenarios. The result is illustrated in Figure 5.5.

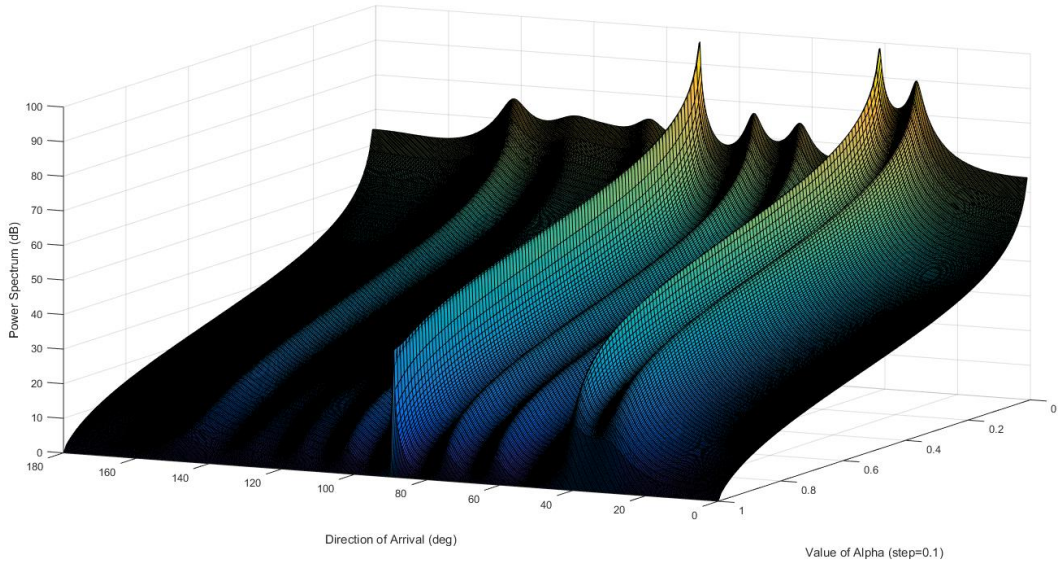

Figure 5.4: The UR-Like Result with Different Alpha Values

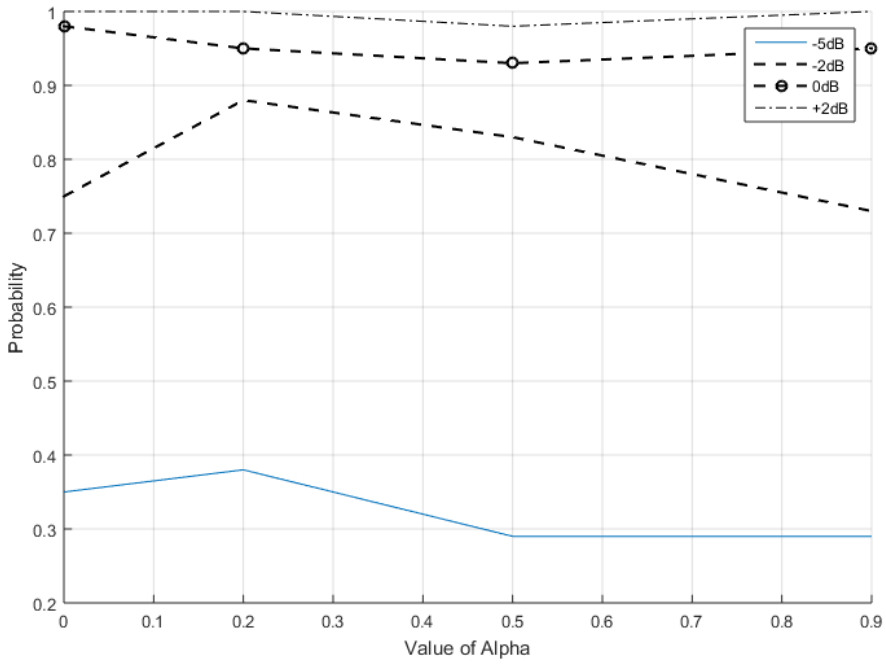

Figure 5.5: Probability of Successful Estimation Against Value of Alpha

The choice of coefficient alpha does not affect the estimation performance significantly in this 3-source-ULA simulation. A larger (larger than 0.5) may degrade the performance. Any small value around 0.2 is acceptable for all the simulations in this report. In all the other simulations related to the UR-Like algorithms in this chapter, the penalty coefficient alpha is set to be 0.2 by default.

5.3.2.4 Performance Comparison Against the MUSIC-Like Algorithm

In Chapter 2, the MUSIC-Like algorithm which is another high-resolution DoA estimation method without the number of sources is introduced. The MUSIC-Like algorithm serves the similar design purpose as the UR-Like algorithm. These two algorithms will be compared in detail.

The design idea of the MUSIC-Like algorithm is inspired by improving the MVDR algorithm. Instead of keeping the array response to unity which reflects the true output signal, the MUSIC-

Like algorithm focusses more on the output power than signal itself. Hence the constraint is the power of array response along with an extra norm constraint term [8]. The constraint of the UR-Like algorithm on the other hand is different. It minimizes the mean-square value of the difference between actual array response and unity response in the interested directions, which is borrowed from the UR algorithm.

A computer simulation is performed to compare these two algorithms. The same 10-element ULA and 3 sources from 30, 40 and 90 degrees are used. The input SNR is 5dB and 100 snapshots are taken.

In terms of estimation performance, both algorithms are able to deliver a high-resolution result in Figure 5.6. Through the resolution capability test shown in Figure 4.7. The UR-Like is even more robust for low SNR scenarios comparing to the MUSIC-Like method.

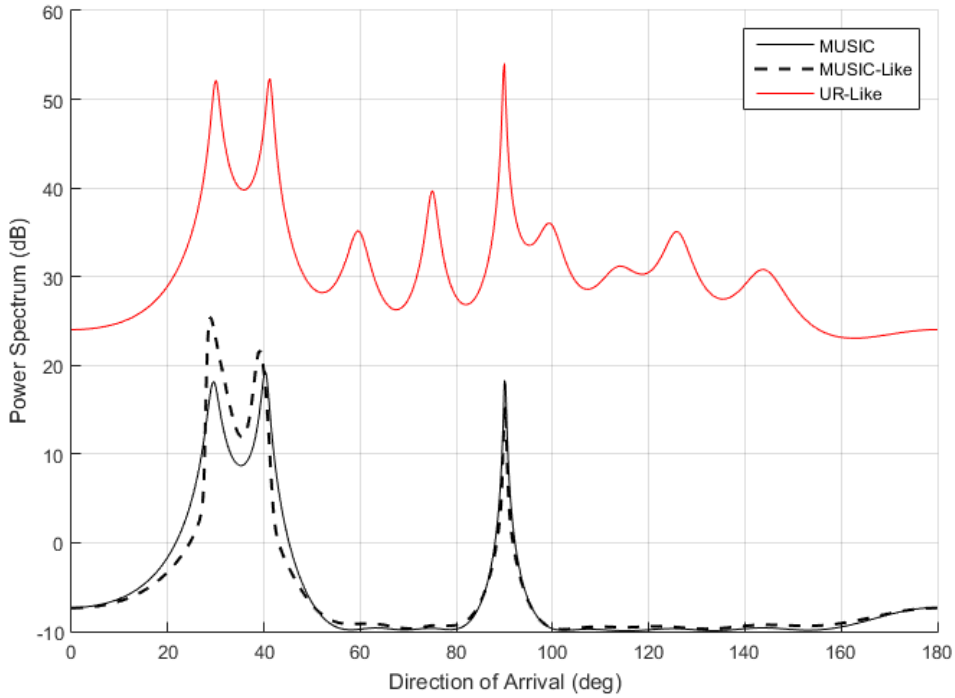

Figure 5.6: The UR-Like versus MUSIC-Like Algorithm Test at SNR = 5dB

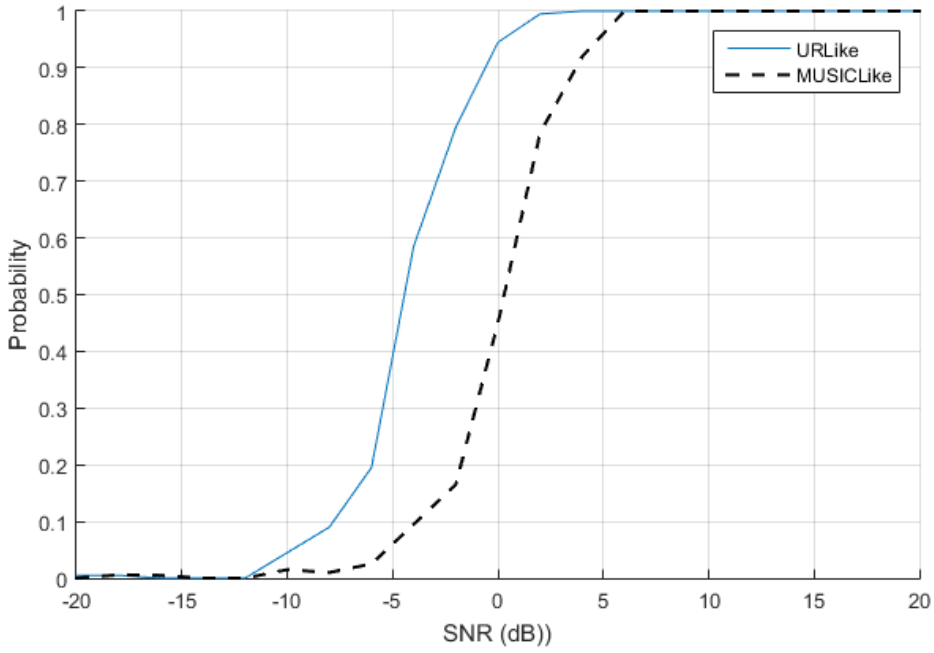

Figure 5.7: Estimation Resolution Probability for the UR-Like and MUSIC-Like Algorithms

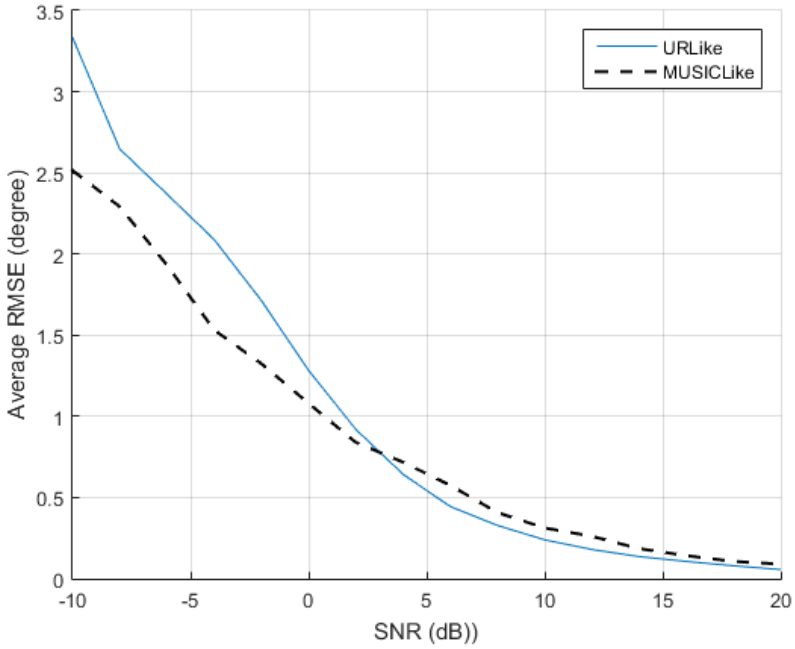

Figure 5.8: RMSE of DoA Estimation Comparison for the UR-Like and MUSIC-Like Algorithms

Moreover, the MUSIC-Like algorithm has a significant drawback which is its computational cost [7]. In order to perform DoA estimation without the number of sources, the MUSIC-Like algorithm solves a generalized eigenvalue problem in each looking direction.

According to the notation definition in Chapter 2, M indicates the number of sensors in the array and N as the number of direction scans across the entire FoV.

For the UR-Like algorithm, the computational load for calculating **Q** and **P** is $O(M^2N)$ and $O(M^3 + 4M^2)$ for the calculation of the weight vector. The beamforming spectrum requires $O(M^2N)$. Hence the total computational load is $O(M^3 + 4M^2 + 2M^2N)$.

For the MUSIC-Like algorithm, the load to compute an appropriate modified covariance matrix is $O(M^2 + M)$. The cost to perform a fast generalized eigen-decomposition is $O(M^2)$. The spectrum requires $O(M^2 + 1)$. All the operations are performed once in each directional scan. Hence the total computational load is $O(3M^2N + MN + N)$.

As a reference, the MVDR algorithm takes $O(M^3)$ to compute the inverse of the data covariance matrix and $O(M^2 + M)$ for the spectrum. The total computational load for the MVDR method is $O(M^3 + M^2N + MN)$.

Assume that the FoV ranges from 0 to 180 degrees, the directional sampling step is 0.5 degree. The total number of directional scan N is 361. The computational complexity versus the number of sensors used for constructing an array is shown in Figure 5.8. In Table 5.3, the computational complexity is compared with respect to 3 different number of directional scans. The number of sensors is fixed to 10. In both scenarios, the UR-Like is less computational heavy comparing to the MUSIC-Like algorithm.

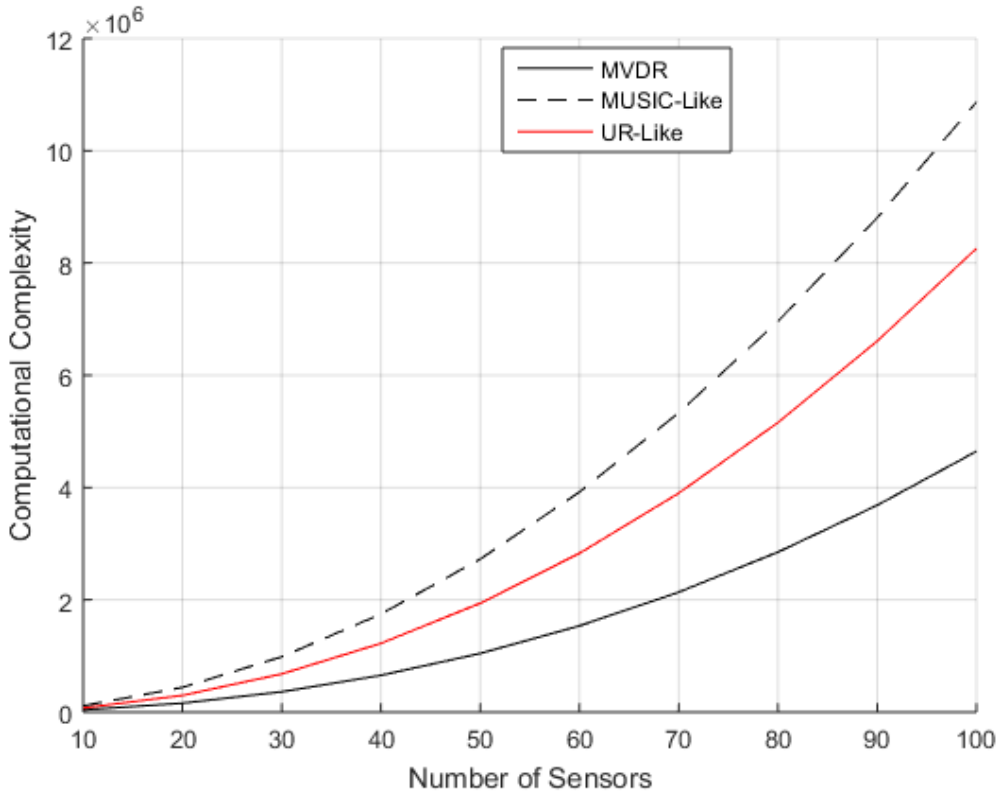

Figure 5.9: Computational Complexity Comparison with respect to Number of Sensors

Number of Scans	MVDR (*10^4)	MUSIC-Like (*10^4)	UR-Like (*10^4)
N = 181 (Step = 1 degree)	2.09	5.63	3.76
N = 361 (Step = 0.5 degree)	4.07	11.23	7.36
N = 1801 (Step = 0.1 degree)	19.91	56.01	36.16

Table 5.3: Computational Complexity Comparison with respect to Number of Scans

5.4 Extending the Penalty Method

The unconstrained minimization problem proposed in Section 5.1 is a new problem that combines MVDR (2.3.18) and UR (2.3.28). There is also one of the reasons why it is called UR-Like. The similar idea could be applied to MVDR (2.3.18) and MUSIC (2.3.24) to form another new minimization problem:

$$\min_{\mathbf{w}} \ \mathbf{w}^H \mathbf{R} \mathbf{w} \tag{5.4.17}$$

$$s.t \ ||\mathbf{w} - \ \mathbf{s}_\theta||^2 = c \, . \tag{5.4.18}$$

There is no hard constraint like (2.3.25) in the MUSIC that requires the eigen-decomposition. Hence the number of sources is no longer necessary in this new problem.

Solving this problem using penalty function approach:

$$\min_{\mathbf{w}} (1-\alpha)\mathbf{w}^H \mathbf{R} \mathbf{w} + \alpha \left|\left|\mathbf{w} - \ \mathbf{s}_\theta\right|\right|^2 . \tag{5.4.19}$$

The solution is obtained as:

$$\mathbf{w}_{MUSIC\_Penalty} = \left((1-\alpha)\mathbf{R} + \alpha \mathbf{I}\right)^{-1} \alpha \mathbf{s}_\theta \, . \tag{5.4.20}$$

The direction-finding function is the array response:

$$DF_{MUSIC\_Penalty} = \mathbf{w}_{MUSIC\_Penalty}^H \mathbf{s}(\theta) = \left((1-\alpha)\mathbf{R} + \alpha \mathbf{I}\right)^{-1} \alpha \mathbf{s}_\theta)^{\,H} \mathbf{s}(\theta) \, . \tag{5.4.21}$$

The computer simulation under the same environment is taken and the figure below shows the result.

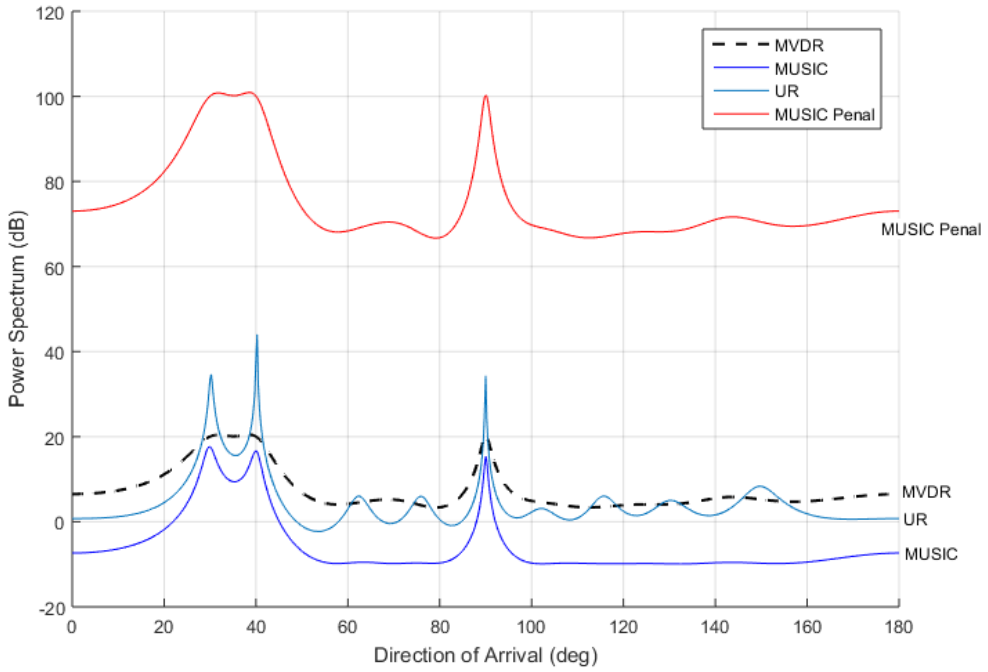

Figure 5.10: MUSIC Principle Penalty Test with Fixed Alpha

The figure shows that this new method using the MUSIC principle (2.3.24) has no improvement compare with the MVDR. The MUSIC principle design is not as effective as the UR-Like design.

5.5 Summary

A new high-resolution DoA estimation method with unknown number of sources is proposed in this chapter, namely the UR-Like algorithm. The UR-Like algorithm delivers similar spatial spectrum as the UR algorithm which has high-resolution but requires the number of sources, and it carries the same phase issue of the UR algorithm.

The UR-Like algorithm is evaluated and compared to other high-resolution algorithms like the UR algorithm, the MUSIC algorithm and the MUSIC-Like algorithm. According to the estimation

probability and RMSE tests, the UR-Like algorithm is able to perform high-resolution DoA estimation with an advantage of unknown number of sources. Comparing to the MUSIC-Like which is also with unknown number of sources, the UR-Like algorithm outperforms it in terms of computational complexity. However, the UR-Like algorithm also faces problems such as the phase issue. Also, its estimation accuracy is sensitive to the input SNR.

The design idea of the UR-Like algorithm is extended in search of new possibilities. Unfortunately, none of the design works well as the UR-Like algorithm. As an inspiration and reference for possible future works, the design and simulation results are presented in Section 5.4.

Chapter 6 DoA Estimation Methods of Wideband Signal Sources

Most of the algorithms discussed, like the MVDR and the MUSIC, are designed and implemented for narrowband signals. In practice, signals usually consist of multiple frequencies or cover a larger frequency bandwidth. In pursuit of a wideband DoA estimation solution, the UR-Like algorithm is extended to fit wideband scenario.

Two methods are applied to the UR-Like algorithms.

6.1 Frequency Scan Method for the UR-Like Algorithm

6.1.1 Formulation

Frequency scan method is an evident approach when extending narrowband algorithms to wideband. The thought is simple. Consider wideband signal as an integration of multiple narrowband signals. Applying the narrowband algorithm to all the narrowband signals would leads to a wideband solution. At first glance, the computational load of this approach is tremendous. N times of weight vector need to be calculated. N represents the number of frequency bands.

However, since the phase shift of wideband signal is frequency sensitive but still holds the superposition theorem for different frequency bands. The steering vector $\mathbf{s}_\theta$ could be reformulated into frequency dependent $\mathbf{s}_{(f,\theta)}$. With the help of the new steering vector, the proposed wideband algorithm requires only one solution for the weight vector throughout the whole estimation.

The working principle is similar to the UR-Like algorithm. Minimize the output power while keep a unity response over the FoV. However, in wideband cases, not only the unity constraint is set in FoV but also in the frequency spectrum. Following such design ideas, the optimization problem is proposed as:

$$\min_{\mathbf{w}} \ \mathbf{w}^H \mathbf{R} \mathbf{w} \tag{6.1.1}$$

$$s.t \ \frac{1}{\Delta f \Delta \theta} \int_f \int_\theta \ |\left|\mathbf{w}^H \mathbf{s}_{(f,\theta)} - \mathbf{1}\right||^2 \, d\theta \, df = c \, . \tag{6.1.2}$$

Similarly, the penalty function method is used to solve this optimization problem:

$$\min_{\mathbf{w}} (1-\alpha)\mathbf{w}^H \mathbf{R} \mathbf{w} + \alpha \frac{1}{\Delta f \Delta \theta} \int_f \int_\theta \ \left|\left|\mathbf{w}^H \mathbf{s}_{(f,\theta)} - \mathbf{1}\right|\right|^2 \, d\theta \, df \, . \tag{6.1.3}$$

The solution of weight vector could be derived as:

$$\mathbf{w}_{Freq\_scan} = \ ((1-\alpha)\mathbf{R} + \alpha \mathbf{Q}) \ ^{-1} \alpha \ \mathbf{P} \, . \tag{6.1.4}$$

where **P** and **Q** are redefined as:

$$\mathbf{Q} = \frac{1}{\Delta f \Delta \theta} \int_f \int_\theta \ \mathbf{s}_{(f,\theta)} \mathbf{s}_{(f,\theta)}^H \, d\theta df \tag{6.1.5}$$

$$\mathbf{P} = \frac{1}{\Delta f \Delta \theta} \int_f \int_\theta \ \mathbf{s}_{(f,\theta)} d\theta df. \tag{6.1.6}$$

Subsequently, the direction-finding function is a function of both bearing angle and signal frequency:

$$DF_{Freq\_scan} = \mathbf{w}_{Freq\_scan}^H \mathbf{s}_{(f,\theta)} = (\ ((1-\alpha)\mathbf{R} + \alpha \mathbf{Q}) \ ^{-1} \alpha \ \mathbf{P}) \ ^H \mathbf{s}_{(f,\theta)} \, . \tag{6.1.7}$$

In narrowband cases, the time delay among all the array sensors is a function of phase delay of the reference signal. According to equation (2.2.4), the steering vector of narrowband only depends on

inter-element-space and incoming signal angel with respect to array axis. In wideband scenarios, the frequency variable is introduced. The new steering vector $\mathbf{s}_{(f,\theta)}$ is a function of the array geometry function related with θ and the signal frequency f. For the same signal received in wideband, the combination of the array geometry function and signal frequency may no longer be unique, which may lead to ambiguous angel estimation for certain frequency. Such combinations are called spurious peaks. Spurious peaks could be minimized by setting up proper array geometry like ring array or wideband structure linear array. Hence is the later simulation part, instead of ULA, a 10-element double-ring array geometry is used. In order to control the presence of spurious peaks furthermore, the signal bandwidth should be limited as well. It is clear to see that the larger the bandwidth is, the more combinations of geometry function and frequency are, which leads to greater probability of spurious set to occur.

6.1.2 Simulation and Evaluation

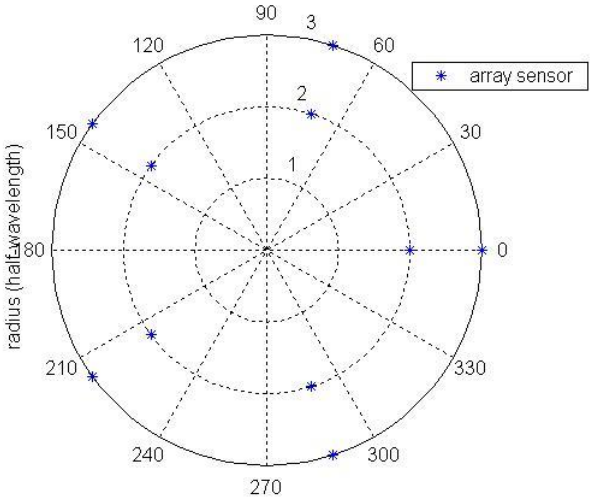

Figure 6.1: Double-ring Sensor Array Geometry

In the computer simulation, a 10-sensor double-ring array geometry is chosen. It is illustrated as Figure 6.1. The three-signal-source scenario covers both wideband and narrowband signals. The signal emitting from 30 degrees covers the frequency band ranging from 80% to 120% of the reference frequency. The signal emitting from 40 degrees covers from 100% to 110% with respect to the reference frequency. The one from 90 degrees is a narrowband signal working on the reference frequency. 100 frames are taken to form the data covariance matrix. SNR is 10 dB. Alpha is set to be 0.2. The frequency scan step is 0.01.

In Figure 6.2, the 3D plot shows the estimation result crosses the maximum frequency band of interest and the whole FoV. In Figure 6.3, the 2D plot is calculated by averaging the array response for the entire frequency band of interest at each bearing angle.

From the simulation result, the signals with different bandwidth can be read from the plot as well as misleading narrowband spurious peaks appearing at angle around 60 and 150 degrees. The signal frequency bandwidth being able to be estimated from the spectrum is an advantage of the frequency scan method. Moreover, throughout the whole process, only one optimal weight vector is calculated which is an improvement for computational cost.

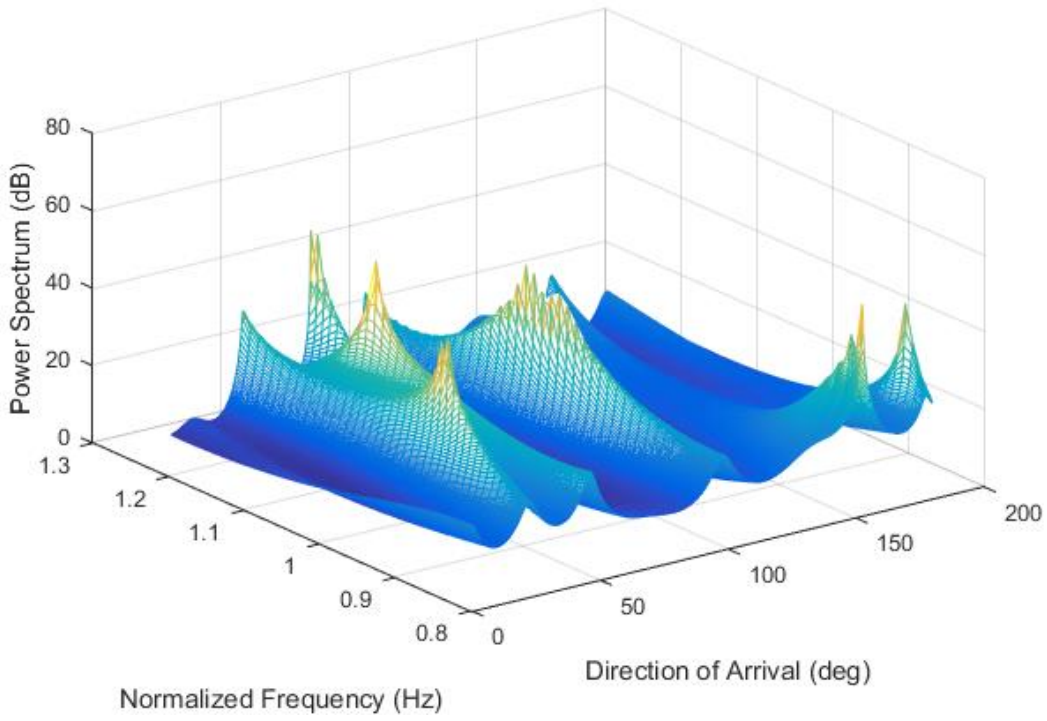

Figure 6.2: Frequency Scan Method for the UR-Like Algorithm Broadband Adoption

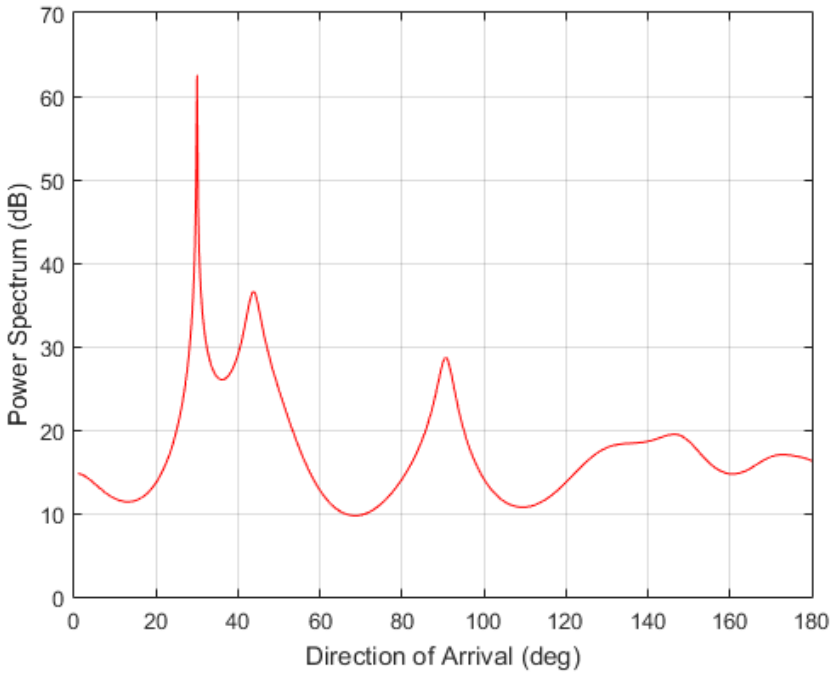

Figure 6.3: Frequency Scan Method for the UR-Like with Averaged Response

However, there are also drawbacks for this method. Firstly, the frequency scan method requires massive computation while plotting the spatial spectrum. For every frequency scan at every scanning angle, there is a direction-finding function calculation. Although the weight vector is computed only once, the computational load is still rather heavy. Secondly, the misleading spurious peaks at angle 60 and 150 degrees appear in the 3D plot. They are attenuated in the 2D plot by averaging the array response across the frequency band. But averaging approach is essentially in favor of the wideband signals. It could cause a poor performance for the narrowband signals. As it is shown in the 2D plot in Figure 6.3, the amplitude of wideband signal from 40 degrees (covers 10% percentage bandwidth with respect to the reference frequency) is not equally high as the that in 30 degrees (covers 40% percentage bandwidth). The narrowband signal at 90 degrees is nearly eliminated and not significant distinguishable from noise.

6.2 Taylor-Series Method for the UR-Like Algorithm

Frequency scan method increases the computational complexity of the UR-Like algorithm. In some cases, only DoA is the matter of concern and the signal bandwidth coverage of the signal is not an information needed. In order to perform a wideband UR-Like algorithm with less computational load and focusing only on DoA, the Taylor-series approach is taken to adopt the UR-Like algorithm to wideband scenarios.

6.2.1 Formulation

Denote the wideband steering vector $\mathbf{s}_{(f,\theta)}$ for a signal at frequency f_i coming from direction θ as $\mathbf{s}_{(f_i,\theta)}$. Expanding $\mathbf{s}_{(f_i,\theta)}$ using the Taylor-series approach:

$$\mathbf{s}_{(f_i,\theta)} = \mathbf{s}_{(f_0,\theta)} + \Delta f \left.\frac{\partial \mathbf{s}_{(f,\theta)}}{\partial f}\right|_{f=f_0} + \frac{\Delta f^2}{2!}\left.\frac{\partial^2 \mathbf{s}_{(f,\theta)}}{\partial f^2}\right|_{f=f_0} + \cdots \tag{6.2.8}$$

where f_0 is the nominal reference frequency and Δf is the difference between f_i and f_0.

An additional constraint is introduced to have null response for frequency f_i and direction θ:

$$\mathbf{w}^H \mathbf{s}_{(f_i,\theta)} \mathbf{s}^H_{(f_i,\theta)} \mathbf{w} = 0\,. \tag{6.2.9}$$

The bandwidth of the UR-Like algorithm could be extended by introducing quadratic equation (6.2.9) into the objective of the optimization problem using soft constraint method.

$$\min_{\mathbf{w}} \ \mathbf{w}^H \mathbf{R} \mathbf{w} + \gamma(\mathbf{w}^H \mathbf{s}_{(f_i,\theta)} \mathbf{s}^H_{(f_i,\theta)} \mathbf{w}) \tag{6.2.10}$$

$$s.t\ \frac{1}{\Delta\theta} \int \left|\left|\mathbf{w}^H \mathbf{s}_{(f_0,\theta)} - \mathbf{1}\right|\right|^2 d\boldsymbol{\theta} = c \tag{6.2.11}$$

where c is a constant and γ is a weight factor which controls the ratio of wideband performance.

From equations (6.2.8) and (6.2.9), the sufficient conditions for the constraint to be valid are:

$$\mathbf{w}^H \mathbf{s}_{(f_0,\theta)} \mathbf{s}^H_{(f_0,\theta)} \mathbf{w} = 0 \tag{6.2.12}$$

$$\mathbf{w}^H \left.\frac{\partial \mathbf{s}_{(f,\theta)}}{\partial f}\right|_{f=f_0} \left.\frac{\partial \mathbf{s}^H_{(f,\theta)}}{\partial f}\right|_{f=f_0} \mathbf{w} = 0 \tag{6.2.13}$$

$$\mathbf{w}^H \left.\frac{\partial^2 \mathbf{s}_{(f,\theta)}}{\partial f^2}\right|_{f=f_0} \left.\frac{\partial^2 \mathbf{s}^H_{(f,\theta)}}{\partial f^2}\right|_{f=f_0} \mathbf{w} = 0 \tag{6.2.14}$$

$$\vdots$$

$$\mathbf{w}^H \left.\frac{\partial^n \mathbf{s}_{(f,\theta)}}{\partial f^n}\right|_{f=f_0} \left.\frac{\partial^n \mathbf{s}^H_{(f,\theta)}}{\partial f^n}\right|_{f=f_0} \mathbf{w} = 0. \tag{6.2.15}$$

The integer *n* is chosen based on the signal bandwidth of interest.

Define:

$$\mathbf{Q} = \frac{1}{\Delta\theta} \int_\theta \mathbf{s}_{(f_0,\theta)} \mathbf{s}^H_{(f_0,\theta)} \, \boldsymbol{d\theta} \tag{6.2.16}$$

$$\mathbf{P} = \frac{1}{\Delta\theta} \int \mathbf{s}_{(f_0,\theta)} \, \boldsymbol{d\theta} \tag{6.2.17}$$

$$\mathbf{R}_i = \mathbf{R} + \gamma \mathbf{s}_{(f_i,\theta)} \mathbf{s}^H_{(f_i,\theta)} = \mathbf{R} + \gamma \mathbf{Q}_i \tag{6.2.18}$$

$$\mathbf{Q}_i = \mathbf{s}_{(f_0,\theta)} \mathbf{s}^H_{(f_0,\theta)} + \left.\frac{\partial \mathbf{s}_{(f,\theta)}}{\partial f}\right|_{f=f_0} \left.\frac{\partial \mathbf{s}^H_{(f,\theta)}}{\partial f}\right|_{f=f_0} + \cdots + \left.\frac{\partial^n \mathbf{s}_{(f,\theta)}}{\partial f^n}\right|_{f=f_0} \left.\frac{\partial^n \mathbf{s}^H_{(f,\theta)}}{\partial f^n}\right|_{f=f_0} \tag{6.2.19}$$

Note that the sufficient conditions for the constraint (6.2.9) to be valid is now translated into $\mathbf{w}^H \mathbf{Q}_i \mathbf{w} = 0$.

Now the optimization problem of the UR-Like algorithm using Taylor series method could be written into:

$$\min_{\mathbf{w}} \ \mathbf{w}^H \mathbf{R}_i \mathbf{w} \tag{6.2.20}$$

$$s.t \ \frac{1}{\Delta\theta} \int \left|\left|\mathbf{w}^H \mathbf{s}_{(f_0,\theta)} - \mathbf{1}\right|\right|^2 \boldsymbol{d\theta} = c. \tag{6.2.21}$$

This problem could be solved using the penalty function method as well and the direction-finding function could be expressed as

$$DF_{URLike\_Taylor} = |\mathbf{w}_{URLike\_Taylor}^H \mathbf{s}_{(f_0,\theta)}| = (\ ((1-\alpha)\mathbf{R}_i + \alpha\mathbf{Q})^{-1} \alpha\ \mathbf{P})^H \mathbf{s}_{(f_0,\theta)}\ . \tag{6.2.22}$$

6.2.2 Simulation and Performance Evaluation

Same 10-sensor double-ring array geometry and 3-source scenario are employed. The signal emitting from 30 degrees covers the frequency band ranging from 80% to 120% of the reference frequency. The signal emitting from 40 degrees covers from 100% to 110% with respect to the reference frequency. The one from 90 degrees is a narrowband signal working on the reference frequency. 100 frames are sampled for the data covariance matrix. SNR is 10 dB.

According to trail simulation results, the integer *n* is selected as 3, which is sufficient for the widest bandwidth of 40%. Gamma is fixed to 0.005 for illustration purpose. The influence of gamma will be discussed later.

From the direction-finding function (6.2.22) and the definition of $\mathbf{R}_i$**,** equation (6.2.18)**,** it is clear that $\mathbf{R}_i$ already contains the information of **Q** which is controlled by factor gamma. Hence the weight factor alpha is actually playing the same role as gamma. To simplify the process, alpha is set to 0 for the UR-Like algorithm broadband adoptions with Taylor series method.

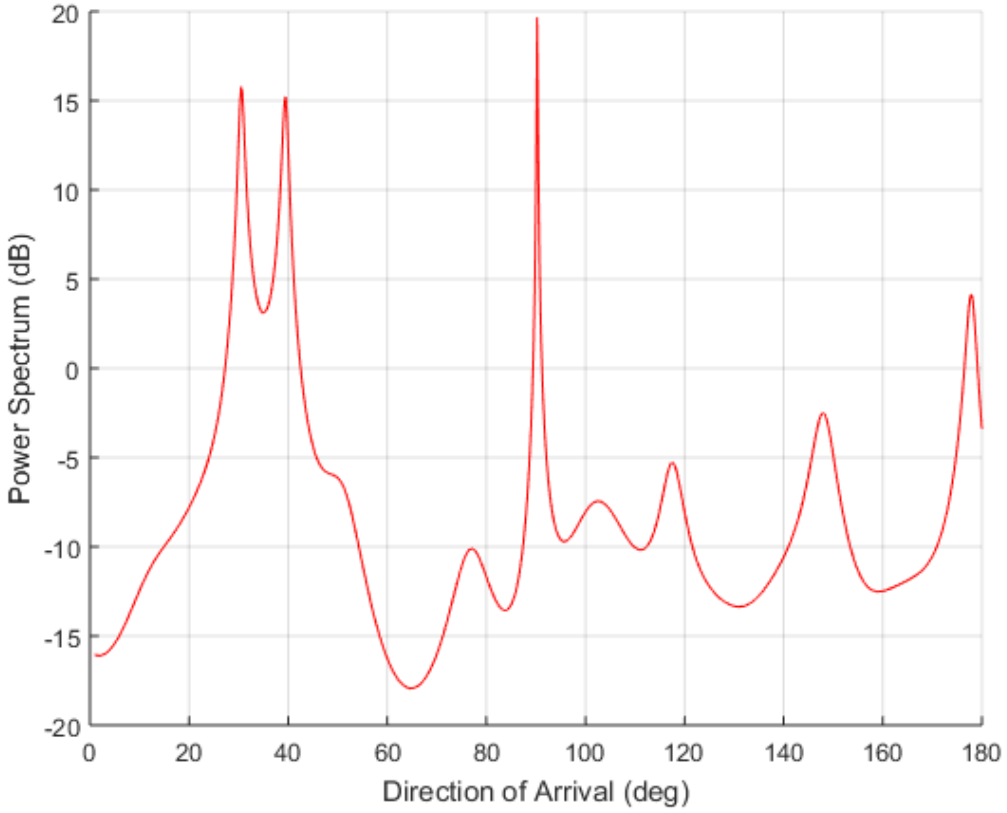

Figure 6.4: Taylor Series Method for the UR-Like Algorithm Broadband Adoption

The figure above shows a successful estimation for all the wideband and narrowband signals. The UR-Like estimator is designed to have flat response at all directions at frequency f_0 while minimizing the output power and frequency f_i as low as possible. If the flat response at frequency f_0 is extended to f_i at a signal direction, the effect of minimization will be brought back and reflected at frequency f_0 spectrum. Therefore, only directional scanning would be enough. Comparing to the frequency scan method, the number of scans is reduced massively. However, due to the additive term $\mathbf{Q}_i$ which changes in every scanning angle, the weight vector for direction-finding function is no longer fixed and cannot be pre-computed once for all. Additional inversion and multiplications are required in each scan.

6.2.3 Discussion

The influence of the value of gamma is illustrated through these two examples. Figures 6.5 and 6.6. When gamma is extremely small ($\gamma = 5 * 10^{-10}$), the algorithm works like a narrowband solution. The performance of power minimization is the best, but the broadband signals are not distinguished. For overpowered large gamma setting ($\gamma = 5$), the broadband signal is estimated clearly. However, the power minimization approach is rather poor. The noise cannot be attenuated properly. For the 3-source setup employed in our simulations, $\gamma = 0.005$ delivers the most balanced result.

For the choice of integer n for the term $\mathbf{Q}_i$, it highly depends on the largest bandwidth of broadband signal of interest. In order to secure f_i in the vicinity of f_0, n must be chosen properly. The basic guideline is that the larger is the bandwidth, the larger is the value of n. For the simulation illustrated in this chapter, $n = 3$ is sufficient for the maximum 40% bandwidth of the reference frequency.

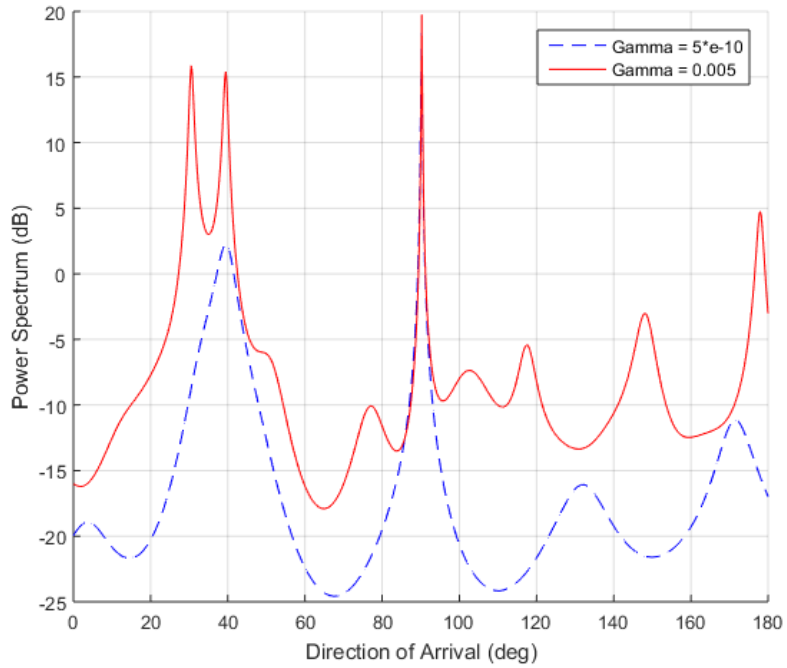

Figure 6.5: Taylor Series Wideband Adoption Method with Small Gamma Values

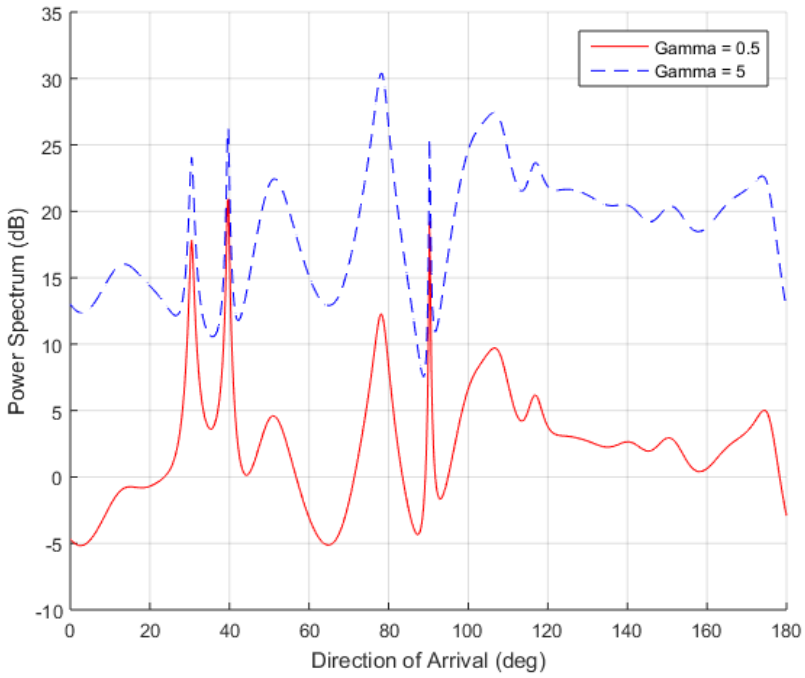

Figure 6.6: Taylor Series Wideband Adoption Method with Large Gamma Values

6.3 Taylor-Series Method Extension

6.3.1 Formulation and Simulation

In Section 6.2, the UR-Like algorithm is adopted to broadband by replacing the data covariance matrix **R** in the objective function with a new version $\mathbf{R}_i$ which is **R** infused with a Taylor series term $\mathbf{Q}_i$. There are two more algorithms which also use output power minimization as objective. Recall the optimization problem for the MVDR algorithm and the MUSIC-Like algorithm.

The MVDR algorithm:

$$\min_{\mathbf{w}} \ \mathbf{w}^H \mathbf{R} \mathbf{w} \tag{2.3.18}$$

$$s.t\ \mathbf{w}^H \mathbf{s}_\theta = 1. \tag{2.3.19}$$

The MUSIC-Like algorithm:

$$\min_{\mathbf{w}} \ \mathbf{w}^H \mathbf{R} \mathbf{w} \tag{2.3.31}$$

$$s.t\ \mathbf{w}^H \mathbf{s}_\theta \mathbf{s}_\theta^H \mathbf{w} + \beta ||\mathbf{w}||^{\mathbf{2}} = c. \tag{2.3.32}$$

By employing similar Taylor series method into those two algorithms, the wideband adoption should be effective as well.

The adopted optimization problems and direction-finding functions are as fellows.

The proposed wideband MVDR algorithm:

$$\min_{\mathbf{w}} \ \mathbf{w}^H \mathbf{R}_i \mathbf{w} \tag{6.3.23}$$

$$s.t\ \mathbf{w}^H \mathbf{s}_{(f_0,\theta)} = 1 \tag{6.3.24}$$

$$DF_{MVDR\_Taylor} = \mathbf{w}^H \mathbf{R}_i \mathbf{w} = \frac{1}{\mathbf{s}^H_{(f_0,\theta)} \mathbf{R}_i^{-1} \mathbf{s}_{(f_0,\theta)}}. \quad (6.3.25)$$

The proposed wideband MUSIC-Like algorithm:

$$\min_{\mathbf{w}} \mathbf{w}^H \mathbf{R}_i \mathbf{w} \quad (6.3.26)$$

$$s.t\ \mathbf{w}^H \mathbf{s}_{(f_0,\theta)} \mathbf{s}^H_{(f_0,\theta)} \mathbf{w} + \beta ||\mathbf{w}||^2 = c \quad (6.3.27)$$

$$DF_{MUSICLike\_Taylor} = \frac{1}{|\mathbf{w}^H_{MUSICLike\_Taylor} \mathbf{s}_{(f_0,\theta)}|^2}. \quad (6.3.28)$$

The 3-source broadband scenario with identical environment settings is performed. $n = 3$ and $\gamma = 0.0005$.

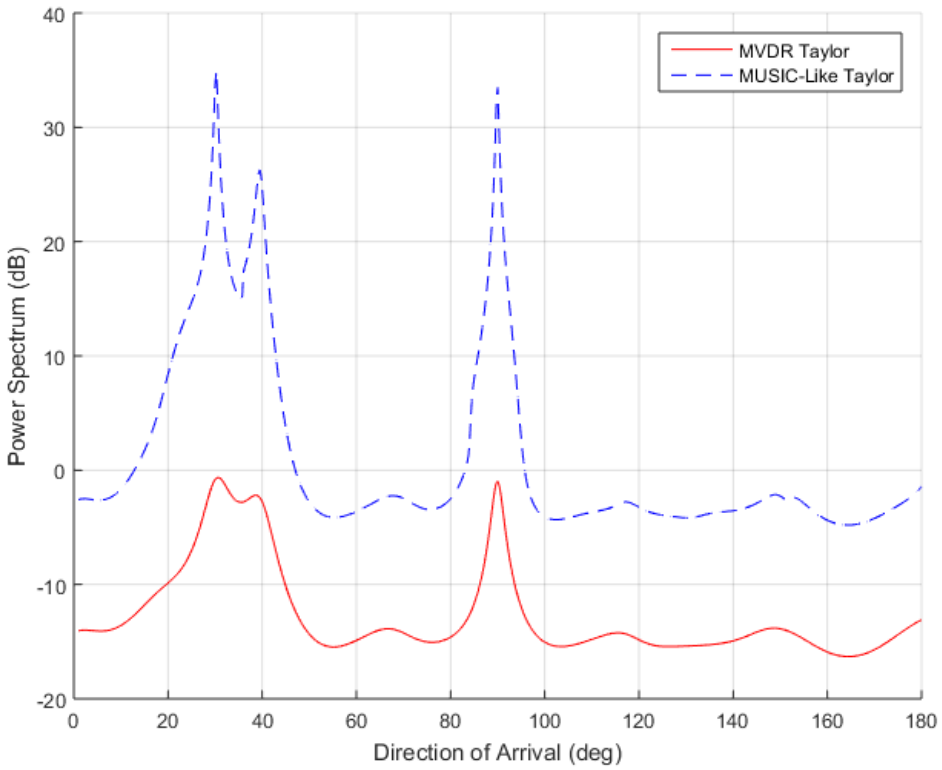

Figure 6.7: Taylor Series Method for the Proposed Wideband MUSIC-Like and MVDR Algorithms

As the figure shows, both the MVDR and the MUSIC algorithms could be extended into broadband cases using the Taylor series method. The reason for 2 detected close-situated signals for the MVDR algorithm is mainly because of the high input SNR.

6.3.2 Discussion

In Figure 6.7, the gamma is set to be 0.0005 for both algorithms. In fact, these two algorithms have different sensitivity against the value of gamma.

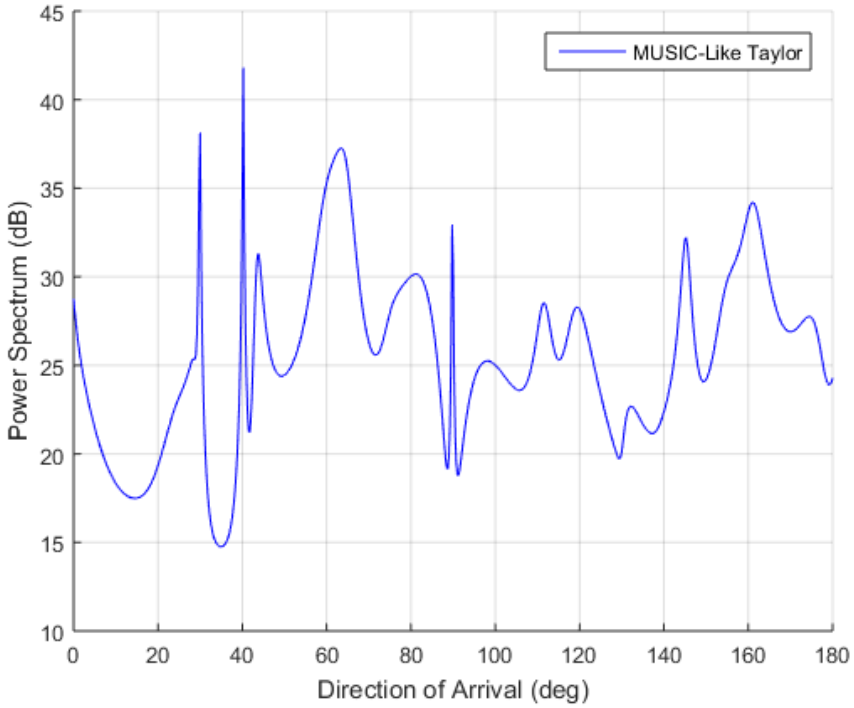

Figure 6.8: The MUSIC-Like algorithm at gamma = 0.5

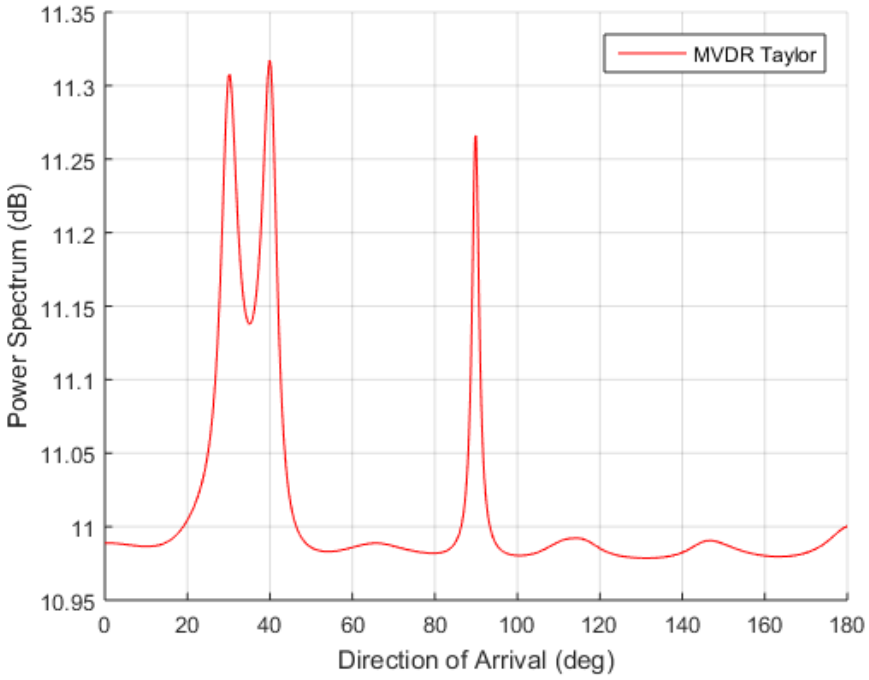

Figure 6.9: The MVDR algorithm at gamma = 50

The MUSIC-Like algorithm distorts heavily when gamma is only 0.5. On the other hand, the MVDR algorithm is still able to deliver meaningful spectrum even at a value of 50. The following tables records the resolution for these two algorithms at different values of gamma.

Gamma Value	0.0005	0.005	0.05	0.5	5	50
Narrowband Resolution (dB)	13	12	11	4	0.7	0.08
Broadband Resolution (dB)	1	2	3	1.5	0.25	0.02

Table 6.1: The Resolution of Broadband MVDR Estimator vs. Different Gamma Values

Gamma Value	0.0005	0.005	0.05	0.5	5	50
Narrowband Resolution (dB)	40	30	5	Unreadable	Unreadable	Unreadable
Broadband Resolution (dB)	10	16	30	Unreadable	Unreadable	Unreadable

Table 6.2: The Resolution of Broadband MUSIC-Like Estimator vs. Different Gamma Values

The broadband MUSIC-Like algorithm already starts to distort when gamma equals 0.05 while the MVDR algorithm is a little bit more robust. The resolution of MVDR algorithm drops significantly for gamma values exceeding 0.05.

With the simulation experience from the UR-Like algorithm, it is safe to claim that gamma value should be taken no more than 0.005 for a meaningful spectrum for the UR-Like, the MUSIC-Like and the MVDR algorithm broadband adoption using the Taylor series method.

Chapter 7 Conclusions and Recommendations

7.1 Conclusions

The wireless communication industry has grown rapidly since the past few decades. 5th Generation of wireless communication technique, Internet of things and Smart Nation strategy have become the reachable applications in real-life. All these techniques or applications require massive signal transmitting and receiving using smart antennas and the techniques behind the antennas. Array signal processing, especially Direction-of-Arrival (DoA) estimation algorithm is one of the major topics.

DoA estimation algorithms are designed to reveal the spatial property of the signal of interest. Many well-known algorithms have been investigated and practically implemented in many applications. Such as Capon's Minimum Variance Distortionless (MVDR) method and Multiple Signal Classification (MUSIC) algorithm. In Chapter 2, the linkage between the MVDR and MUSIC algorithm is revealed. The MUSIC algorithm could be interpreted as a MVDR estimator with infinite input SNR. With the information of number of sources, eigen-decomposition is employed in the MUSIC algorithm. The interpretation becomes real after applying subspace techniques. This linkage also reveals the struggle of balance among estimation resolution, information needed and computational load. Number of sources is required and extra eigen-decomposition is needed as the cost of high-resolution result of the MUSIC algorithm.

Inspired by the MVDR interpretation of the MUSIC algorithm, an alternative algorithm is design as a MVDR estimator with negative infinite noise amplitude, which also leads to infinite SNR. The alternative high-resolution algorithm proves similar result as the MUSIC algorithm. Instead of setting the signal amplitude to infinite which causes distortion in the output signal power, the

alternative algorithm keeps the true signal power. Its spatial spectrum could provide the signal amplitude information which the MUSIC estimator could not.

During the study of the linkage between the MVDR and MUSIC algorithm, a nature of the MUSIC algorithm is discovered. The shape of signal peak in the spatial spectrum of the MUSIC estimator is the function of number of array elements and is independent from the signal environment. This nature is the basic of the proposed improved scanning method in Chapter 4. The improved scanning method uses two experience mathematical estimation models to predict the shape of signal peaks in the spectrum. The improved method only scans the direction range with signal peak potential and skips the range of noise. The total number of scans is reduced with the help of the improved scanning method, so as the computational complexity of the MUSIC estimator. The computational load is reduced at least 50% in the computer simulations without any detection miss or resolution degradation.

In Chapter 2, the MUSIC-Like algorithm is studied. The design idea of the MUSIC-Like algorithm is inspired by improving the MVDR method. The MUSIC-Like redesigns the constraint in the MVDR optimization problem. In Chapter 5, a similar idea is applied to proposition of a new high-resolution technique without number of sources, the UR-Like algorithm. The constraint of the UR-Like algorithm minimizes the mean-square value of the difference between actual array response and unity response in the interested directions, which is borrowed from the UR algorithm. The optimization problem of the UR-Like algorithm is solved by applying penalty function method and the result is very close to the UR algorithm with an improvement of not using the information of number of sources. The UR-Like algorithm is examined in detail for its performance, especially against the other high-resolution algorithm without number of sources, the MUSIC-Like algorithm. Simulation shows that the UR-Like algorithm has the advantage in computational complexity and low SNR robustness against the MUSIC-Like algorithm, but less precise in terms of estimation

accuracy. The attempts to extend the idea of improving the MVDR estimator with different constraints are tried as well. However, the result is not ideal.

The UR-Like algorithm is designed successfully in narrowband template. But in real-life applications, signals may contain serval frequency components. In Chapter 6, the UR-Like is extended to broadband scenarios. Firstly, a trivial frequency scan method is implemented. It is designed to perform 2-D scanning in both directional and frequency range. The 3-D spectrum reveals not only the DoA but also the frequency band range of the signal sources. Although the frequency scan method is design to estimated only one weight vector for all the 2-D scans, the massive number of scanning still brings tremendous computational load. Moreover, the frequency scan method is limited to certain array geometries and maximum frequency bandwidth. The second method implemented is the Taylor series method. It requires only the directional scanning, which is less computational heavy comparing to the frequency scan method. The 2-D result of the Taylor series method could not reveal the signal frequency bandwidth but the most important DoA information is estimated precisely. Since the design nature of the MVDR, the MUSIC-Like and the UR-Like algorithm is linked, the Taylor series method is also applied to the MVDR and the MUSIC-Like algorithm for broadband adoption.

7.2 Recommendations for Future Research

Due to limited time and energy, there are still topics could possibly be researched and studied in the future besides all the content concluded in Section 7.1.

In Chapter 3, the alternative high-resolution algorithm still faces stability issues. The clips could be smoothened by applying moving average filter. However, the problem is not solved from the root, which left room for future work.

In Chapter 5, the modified-MVDR design template is studied by applying the MUSIC principle. The constraint is directly borrowed from the MUSIC algorithm. However, the result shows no improvement. It is reasonable to modify the MUSIC principle constraint for a better high-resolution result in the future work.

One important note to remark is that the optimization problems are designed focusing on uncorrelated signal sources scenarios. All the simulations performed in this thesis, the signal sources are uncorrelated signals as well. When it comes to correlated or coherent signal sources, the validation and adoption for all the proposed DoA estimation method needs to be done.

Bibliography

[1] L. Godara, "Application of antenna arrays to mobile communications. II. Beam-forming and direction-of-arrival considerations", *Proceedings of the IEEE*, vol. 85, no. 8, pp. 1195-1245, 1997.

[2] B. van Veen, "Minimum variance beamforming with soft response constraints", *IEEE Transactions on Signal Processing*, vol. 39, no. 9, pp. 1964-1972, 1991.

[3] S. Reddi, "Multiple Source Location-A Digital Approach", *IEEE Transactions on Aerospace and Electronic Systems*, vol. -15, no. 1, pp. 95-105, 1979.

[4] B.P. Ng, M.H. Er and C. Kot, "A MUSIC approach for estimation of directions of arrival of multiple narrowband and broadband sources", *Signal Processing*, vol. 40, no. 2-3, pp. 319-323, 1994.

[5] B.P. Ng, "Bearing estimation using unity response beamforming approach", *IEEE Proceedings H Microwaves, Antennas and Propagation*, vol. 138, no. 6, p. 537, 1991.

[6] V. Reddy, M. Mubeen and B.P. Ng, "Reduced-Complexity Super-Resolution DOA Estimation with Unknown Number of Sources", *IEEE Signal Processing Letters*, vol. 22, no. 6, pp. 772-776, 2015.

[7] Ying Zhang and Boon Poh Ng, "MUSIC-Like DOA Estimation Without Estimating the Number of Sources", *IEEE Transactions on Signal Processing*, vol. 58, no. 3, pp. 1668-1676, 2010.

[8] V. Reddy, B. Ng and A. Khong, "Insights Into MUSIC-Like Algorithm", *IEEE Transactions on Signal Processing*, vol. 61, no. 10, pp. 2551-2556, 2013.

[9] Joseph C. Liberti, JR. and Theodore S. Rappaport, “Smart Antennas for Wireless Communications: IS-95 and third generation CDMA applications,” *Prentice Hall PTR*, 1999